Journal of Medicinal Chemistry

Article

Application of a Parallel Synthetic Strategy in the Discovery of Biaryl Acyl Sulfonamides as Efficient and Selective Na1.7 Inhibitors

Erin F. DiMauro, Stephen Altmann, Loren M. Berry, Howard Bregman, Nagasree Chakka, Margaret Chu-Moyer, Elma Feric Bojic, Robert S. Foti, Robert T. Fremeau, Jr., Hua Gao, Hakan Gunaydin, Angel Guzman-Perez, Brian E. Hall, Hongbing Huang, Michael Jarosh, Thomas Kornecook, Josie Lee, Joseph Ligutti, Dong Liu, Bryan D. Moyer, Daniel Ortuno, Paul E. Rose, Laurie B Schenkel, Kristin Taborn, Jean Wang, Yan Wang, Violeta L. Yu, and Matthew M. Weiss

J. Med. Chem., **Just Accepted Manuscript** • DOI: 10.1021/acs.jmedchem.6b00425 • Publication Date (Web): 21 Jul 2016

Just Accepted

ACS Publications

Journal of Medicinal Chemistry is published by the American Chemical Society. 1155 Sixteenth Street N.W., Washington, DC 20036

Application of a Parallel Synthetic Strategy in the Discovery of Biaryl Acyl Sulfonamides as Efficient and Selective $Na_V1.7$ Inhibitors

Erin F. DiMauro*[,†], Stephen Altmann[§,┤], Loren M. Berry[‡], Howard Bregman[†], Nagasree Chakka[†], Margaret Chu-Moyer[†], Elma Feric Bojic[§,┤], Robert S. Foti[‡], Robert Fremeau[§,┤], Hua Gao[I], Hakan Gunaydin[I,┤], Angel Guzman-Perez[†], Brian E. Hall[±], Hongbing Huang[†,┤], Michael Jarosh[§], Thomas Kornecook[§], Josie Lee[§], Joseph Ligutti[§], Dong Liu[§], Bryan D. Moyer[§], Daniel Ortuno[§,┤], Paul E. Rose[±], Laurie B. Schenkel[†], Kristin Taborn[§], Jean Wang[§], Yan Wang[±], Violeta Yu[§], and Matthew M. Weiss[†]

[†]Department of Medicinal Chemistry, [I]Department of Molecular Engineering, [‡]Department of Pharmacokinetics and Drug Metabolism, [§]Department of Neuroscience, and [±]Department of Biologics, Amgen Inc., 360 Binney Street, Cambridge, Massachusetts 02142, and One Amgen Center Drive, Thousand Oaks, CA 91320, United States.

ABSTRACT

The majority of potent and selective $hNa_V1.7$ inhibitors possess common pharmacophoric features that include a heteroaryl sulfonamide headgroup and a lipophilic aromatic tail group. Recently, reports of similar aromatic tail groups in combination with an acyl sulfonamide headgroup have emerged, with the acyl sulfonamide bestowing levels of selectivity over $hNa_V1.5$ comparable to the heteroaryl sulfonamide. Beginning with commercially available carboxylic acids that met selected pharmacophoric requirements in the lipophilic tail, a parallel synthetic approach was applied to rapidly generate the derived acyl sulfonamides. A biaryl acyl

sulfonamide hit from this library was elaborated, optimizing for potency and selectivity with attention to physicochemical properties. The resulting novel leads are potent, ligand and lipophilic efficient, and selective over $hNa_V1.5$. Representative lead **36** demonstrates selectivity over other human Na_V isoforms and good pharmacokinetics in rodents. The biaryl acyl sulfonamides reported herein may also offer ADME advantages over known heteroaryl sulfonamide inhibitors.

INTRODUCTION

Aberrant action potential firing of nociceptive neurons can lead to pain. The fast upstroke of the action potential is produced by entry of sodium ions through voltage-gated sodium channels (Na_V).[1] There are nine different isoforms of voltage-gated sodium channels ($Na_V1.1$ – $Na_V1.9$), which have distinct expression patterns in neurons, cardiac muscle and skeletal muscle.[2] Non-selective Na_V inhibitors such as lidocaine, mexiletine, and carbamazepine show clinical efficacy in chronic pain, but are limited in dose and in use, likely due to effects on other Na_V isoforms outside of the pain pathway.[3] The tetrodotoxin-sensitive (TTX-S) voltage-gated sodium channel 1.7 ($Na_V1.7$) encoded by the SCN9A gene, is required to sense pain in humans and mice.[4] Rare genetic forms of severe chronic pain, primary erythromelalgia (PE) and paroxysmal extreme pain disorder (PEPD), result from mutations that increase the activity of $hNa_V1.7$.[5] Conversely, the root cause of the genetic disorder congenital insensitivity to pain (CIP) is a loss of function mutation of $hNa_V1.7$.[6] These studies indicate that $hNa_V1.7$ is critical for human pain perception. Additionally, human and mouse genetics highlight a critical role of Nav1.7 in itch. A human $Na_v1.7$ gain of function mutation leads to both paroxysmal itch and pain,[7] whereas $Na_v1.7$ knockout mice show no withdrawal responses to painful stimuli or scratching responses to histamine.[4c] Accordingly, a small molecule therapeutic agent that

selectively inhibits hNa$_V$1.7 should effectively treat pain or itch in humans. Several contemporary reviews summarize progress in the quest for potent and selective small molecule inhibitors of hNa$_V$1.7.[8] In recent years, we and others have focused on identifying novel and advantageous leads from within the heteroaryl sulfonamide class of inhibitors that was originally pioneered by Pfizer/Icagen,[9] and later advanced by Genentech/Xenon,[10] as these routinely demonstrate high levels of potency and selectivity over the human cardiac sodium channel 1.5 (hNa$_V$1.5). In a complementary fashion, we embarked on a secondary pursuit to discover a novel and structurally distinct class of inhibitors that could demonstrate similar potency and selectivity, coupled with improved efficiency and favorable ADME properties.

RESULTS AND DISCUSSION

In 2012, the first acyl sulfonamide hNa$_V$1.7 inhibitors were disclosed by Pfizer.[11] Representative acyl sulfonamides **1** and **2** were determined to inhibit hNav1.7 with selectivity over hNa$_V$1.5 in Patch-Xpress (PX) electrophysiological assays[12] and human ether-a-go-go related gene (hERG) in a [^{3}H]dofetilide displacement[13] assay (Table 1). A comparison to 6,6-fused heteroaryl sulfonamide leads developed at Amgen[14] was made on the basis of potency, selectivity, ligand efficiency (LE), lipophilic efficiency (LipE),[15,16] and pK_a,[16] using representative sulfonamide **3**.[14] Initial data for our heteroaryl sulfonamide series suggested the potential for transporter-mediated clearance, specifically in regard to the organic anion-transporting polypeptide (OATP) transporters.[14a, 17] Under the hypothesis that the heteroaryl sulfonamide headgroup was a recognition element for hepatic drug transporters such as OATP, it was envisioned that the acyl sulfonamides, possessing an alternative pharmacophore and slightly different pK_a, may be cleared by a different mechanism, and thereby offer a potentially advantageous ADME profile. Furthermore, the accumulation of internal data on sulfonamides

had alerted us to a tendency towards undesirable increases in molecular weight and lipophilicity in the quest for potency, leading to issues with selectivity over inhibition of CYP isoforms (particularly 2C9) or induction of CYPs via PXR activation. With respect to efficiency, the acyl sulfonamides **1** and **2** generally compared favorably to our early heteroaryl sulfonamide leads, and a strategy that specifically focused on lipophilic efficiency from the outset of lead discovery was envisioned to be advantageous for delivering metabolically stable leads with minimal safety risks.

Table 1. Representative Pfizer acyl sulfonamide and Amgen heteroaryl sulfonamide $hNa_V1.7$ inhibitors[a]

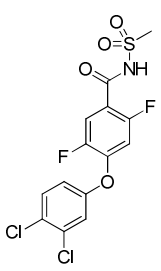

1

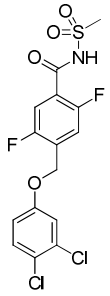

2

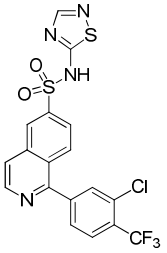

3

Cmpd	**1**	**2**	**3**
$hNa_V1.7$ IC_{50} (μM)[b]	0.74	0.076	0.59
$hNa_V1.5$ IC_{50} (μM)[c]	>30	11	27
hERG K_i (μM)	>30	>30	2.0
LE / LipE[d]	0.35 / 4.83	0.39 / 5.84	0.28 / 4.57
pK_a[e]	3.37	3.41	3.62

[a] Reported data was collected at Amgen. [b] $hNa_v1.7$ data were collected using a PatchXpress automated electrophysiology platform using a protocol where cells were held at a voltage yielding 20-50% channel inactivation. [c] $hNa_v1.5$ data were collected on the same platform using a protocol where cells were held at -50 mV. [d] LipE was calculated using $hNa_V1.7$ PX IC_{50} and Amgen $Na_V1.7$ project cLogD(7.4), which was calculated using daylight cLogP and an Amgen pK_a calculator. [e] Amgen pK_a

calculator was based on an empirical statistical in silico model derived using the Cubist statistical method and a pool of 820 molecular descriptors.

A conformational analysis and molecular overlay of inhibitors **1**, **2** and **3** was performed (Scheme 1). On the basis of this overlay, it was anticipated that the acquired wealth of SAR from our internal efforts on heteroaryl sulfonamides possessing 6,6-fused aryl cores related to **3**,[14] might be applied towards the rapid generation of novel acyl sulfonamide leads with high efficiency. Thus, the acyl sulfonamide headgroup was grafted onto our established 6,6-fused aryl cores. While the resulting 6,6-fused aryl analogs, such as isoquinoline **4**, were only weakly potent, the incorporation of an O-linker between the isoquinoline and phenyl rings afforded significantly enhanced potency, as exemplified by **5**. Further elaboration of the bottom aryl ring with a focus on driving potency and LipE delivered moderately improved pyridyl leads, such as **6**, which exhibited reasonably good potency, selectivity over $hNa_V1.5$, low intrinsic clearance in liver microsomes (HLM, RLM CL_{int}: 17, < 14 μL/min/mg), and high solubility (PBS pH 7.4: 486 μM, FaSSIF pH 6.8: 462 μM). Since heteroaryl sulfonamides have suffered from CYP inhibition issues,[10] we evaluated acyl sulfonamide lead **6** for inhibitory activity on hCYP3A4, 2D6 and 2C9 isoforms in both standard and time-dependent assays (Table 2).[18] Compound **6** displayed significant inhibitory activity on CYP3A4 and 2C9, and was therefore not ideally suited for further optimization. Furthermore, while leads **5** and **6** afforded LipE >5 and >40-fold selectivity over hNav1.5, the observation that smaller, more flexible ethers such as **1** had LipE = 5.8 and selectivity of 144-fold, led us to speculate that the rigid 6,6-core might not be a competitive starting point for lead optimization. Finally, we sought to identify a novel, but more modular core system, wherein rapid synthetic chemistry would allow for SAR exploration in divergent directions.

Scheme 1. Evolution of isoquinoline acyl sulfonamides[a]

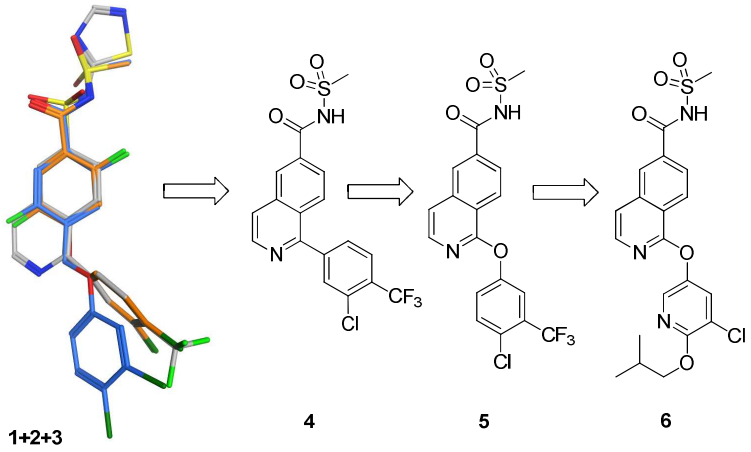

Cmpd	**4**	**5**	**6**
$hNa_V1.7$ IC_{50} (μM)[b]	1.55	0.28	0.20
$hNa_V1.5$ IC_{50} (μM)[c]	>30	14.4	8.7
hERG K_i (μM)	>30	>30	>30
LE / LipE[d]	0.28 / 4.25	0.31 / 5.01	0.31 / 5.23

[a] Deprotonated species - **1** orange; **2** blue; **3** gray. Full conformational analyses were conducted with MMFF94, followed by a rigid body alignment of the conformers with lowest energy in MOE. [b] hNav1.7 data were collected using a PatchXpress automated electrophysiology platform using a protocol where cells were held at a voltage yielding 20-50% channel inactivation. [c] hNav1.5 data were collected on the same platform using a protocol where cells were held at -50 mV. [d] LipE was calculated using $hNa_V1.7$ PX IC_{50} and Amgen $Na_V1.7$ project cLogD(7.4), which was calculated using daylight cLogP and an Amgen pK_a calculator.

Table 2. hCYP Inhibitory activity of **6**

hCYP	3A4	2D6	2C9
IC_{50} (μM)[a]	30.7	>50	9.4
Shifted IC_{50} (μM)[b]	18.4	>50	11.1

[a] Compound **6** was co-incubated with probe substrate of enzyme activity. [b] Compound **6** was pre-incubated with enzyme and co-factor for 30 minutes prior to addition of probe substrate to determine potential for time-dependent inhibition.

Accordingly, an unbiased parallel synthetic strategy was adopted to identify leads with novel and efficient cores, beginning with commercially available carboxylic acids possessing a preferred 3,4-dichlorophenyl ring connected via any type of linker to the carboxylate group. A diverse library of acyl sulfonamides was prepared in parallel, using a single coupling reaction followed by high throughput parallel purification and characterization (HT-LC/MS, HT-NMR). Using this strategy, weakly potent biaryl lead **7a** was identified. The majority of other products from this library did not significantly inhibit hNav1.7 (< 5% at 5 μM; See SI Table S1 for a comprehensive table of products **7b-t**). Lead **7a** was rapidly elaborated to **8** and **9**, both of which showed improved potency and LipE, while maintaining high selectivity. The marked substituent effects on the top aryl ring suggested that a further increase in potency could be realized via exploration of this region of the scaffold. Furthermore, lead **9** was promising from the standpoint of minimal observed CYP inhibition (Table 3) and the 2-alkoxy pyridyl moiety offered a convenient retrosynthetic disconnect for exploration of tail group SAR using parallel S_NAr chemistry.

Scheme 2. Evolution of biaryl acyl sulfonamides

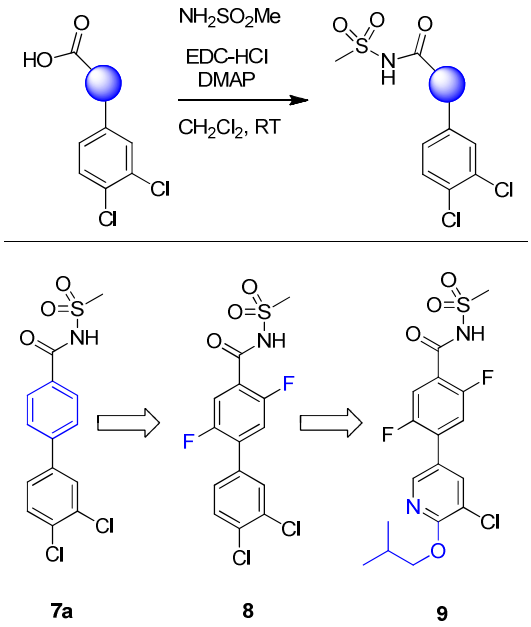

7a **8** **9**

Cmpd	**7a**	**8**	**9**
$hNa_V1.7$ IC_{50} (μM)[a]	10.7	2.54	0.53
$hNa_V1.5$ IC_{50} (μM)[b]	>42	>42	>30
hERG Ki (μM)	>30	>30	>30
LE / LipE[c]	0.32 / 3.65	0.33 / 4.30	0.32 / 4.98

[a] hNav1.7 data were collected using a PatchXpress automated electrophysiology platform using a protocol where cells were held at a voltage yielding 20-50% channel inactivation. [b] hNav1.5 data were collected on the same platform using a protocol where cells were held at -50 mV. [c] LipE was calculated using $hNa_V1.7$ PX IC_{50} and Amgen $Na_V1.7$ project cLogD(7.4), which was calculated using daylight cLogP and an Amgen pK_a calculator.

Table 3. hCYP Inhibitory activity of **9**

hCYP	3A4	2D6	2C9
IC_{50} (μM)[a]	>50	>50	34.1
Shifted IC_{50} (μM)[b]	48.6	>50	34.7

[a] Compound **9** was co-incubated with probe substrate of enzyme activity. [b] Compound **9** was pre-incubated with enzyme and co-factor for 30 minutes prior to addition of probe substrate to determine potential for time-dependent inhibition.

Having identified **9** as a promising lead with a novel and modular biaryl core, with a favorable CYP inhibition profile relative to **6**, we set out to optimize the substitution pattern on the top aryl ring. Table 4 describes selected SAR in this portion of the molecule. C-2 was found to be generally intolerant to substitution (R^1), as substantial potency loss was observed with groups larger than H and F (e.g., R^1=Me, **13** and R^1=Cl, **14**). C-3 (A) was similarly intolerant to substitution. A 2-fold loss in potency and a significant loss in selectivity were observed with A = CF (**15** vs. **11**), and a 16-fold potency loss was observed when CH was replaced with N (**16** vs. **11**). In contrast, C-5 was broadly tolerant to substitution (R^2), with a variety of small lipophilic groups or rings affording compounds of comparable potency (**17**-**20**). However, increased lipophilicity or size at this position generally corresponded with a substantial decrease in human microsomal stability. Introduction of some polarity at C-5 was well tolerated with ethers, such as dihydrofuran **19** and methoxy **21**, while also realizing high selectivity. However, some potency loss was observed upon increasing polarity (e.g., nitrile **22**), and larger, highly polar substituents such as dimethylamide were not well tolerated (**23**). Ultimately, we opted to proceed with 5-OMe phenyl (**21**) as the near optimal top ring on the basis of its modest advantages with respect to potency, lipophilic efficiency, and microsomal stability.

Table 4. Selected SAR of the top aryl ring

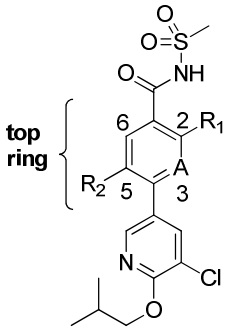

Cmpd	R^1, R^2, A	$hNa_V1.7$[a]	$hNa_V1.5$[b]	HLM / RLM	LipE[c]

		IC_{50} (μM)	IC_{50} (μM)	CL_{int} (μL/min/mg)	
9	F, F, CH	0.53	> 30	47 / 22	4.98
10	F, H, CH	3.04	18	< 14 / 28	4.36
11	H, F, CH	0.66	23	27 / 22	4.66
12	H, H, CH	1.19	32	14 / < 14	4.57
13	Me, H, CH	> 42	N.D.	22 / < 14	--
14	Cl, H, CH	> 42	N.D.	26 / < 14	--
15	H, F, CF	1.24	5.2	22 / <14	4.24
16	H, F, N	10.6	N.D.	18 / 18	4.25
17	H, Cl, CH	0.29	9.5	30 / 16.5	4.74
18	H, CF_3, CH	0.27	3.1	> 399 / < 14	4.35
19	H, 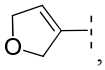 , CH	0.26	> 42	> 399 / < 14	5.63
20	H, OCF_3, CH	0.14	3.7	> 399 / < 14	4.84
21	H, OMe, CH	0.35	> 30	44 / 32	5.39
22	H, CN, CH	1.62	24	20 / < 14	4.81
23	H, $CONMe_2$, CH	> 42	N.D.	19 / < 14	--

[a] hNav1.7 data were collected using a PatchXpress automated electrophysiology platform using a protocol where cells were held at a voltage yielding 20-50% channel inactivation. [b] hNav1.5 data were collected on the same platform using a protocol where cells were held at -50 mV. [d] N.D. = not determined. [c] LipE was calculated using $hNa_V1.7$ PX IC_{50} and Amgen $Na_V1.7$ project cLogD(7.4), which was calculated using daylight cLogP and an Amgen pK_a calculator.

With the top aryl ring fixed as 5-methoxy phenyl, a second parallel synthetic strategy was applied to explore SAR at the bottom ring and linker. Taking advantage of the convenient synthetic handle afforded by the chloro-pyridyl central ring, intermediate **24** (Table 5) was rapidly generated on scale, using readily available building blocks and two synthetic steps.

Broad SAR explorations of both the linker (L = O, S, NR') and bottom substituents (R) were then conducted using the appropriate S_NAr reactions, followed by high throughput parallel purification and characterization with HT-LC/MS and HT-NMR. These libraries were designed using virtual enumeration, with ranking and scoring of virtual targets based on calculated cLogD, PSA, and predicted CL_{int} in LM. In this manner, a vast assortment of diverse compounds was quickly generated and tested for biological activities. Selected SAR from this effort is shown in Table 5.

A variety of bottom substituents (R) and linkers (L) were tolerated, with an ether linker in combination with a ring-containing substituent affording the best balance of lipophilic efficiency, selectivity and microsomal stability. Ethers containing 2-3 small lipophilic substituents (Cl, Me, CF_3, OCF_3) arranged in a variety of substitution patterns around a phenyl ring proved to be the most potent compounds (e.g., **25**). Bis-fluorinated phenyl rings such as **26** were moderately potent and efficient. Substituted pyridyl methoxy ethers lent a boost in lipophilic efficiency with a modest loss of potency (e.g., **27**). Substituted benzylic ether leads with good potency, selectivity, and efficiency were also identified (e.g., **28**). Weakly potent leads containing small, branched alkyl and cycloalkyl ethers were considered advantageous due to their relatively high ligand and lipophilic efficiency (e.g., **29** and **30**), though modest potency and/or high intrinsic clearance in HLM (**30**) prevented these leads from advancing. Moderately potent compounds containing phenyl thioethers (e.g., **31**) and secondary amines (e.g., **32**) were discovered, but these generally suffered a loss in human microsomal stability. Leads emerging from this library effort that met established criteria for potency (Nav1.7 IC_{50} < 0.075 μM), selectivity (>100 fold over hNav1.5), and RLM CL_{int} (< 30 μL/min/mg) were advanced to rat IV PK studies. As such,

compound **25** (CL = 0.56 L/h/kg) was deemed favorable and was thus used as a point of reference for exploration of middle ring Cl replacement SAR.

Table 5. Selected SAR of the bottom substituent (R) and linker (L)

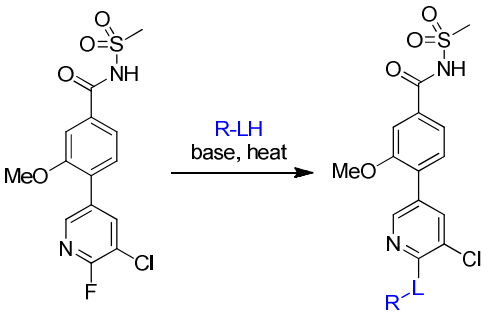

24 **25-32**

Cmpd	-LR	$hNa_V1.7$[a] IC_{50} (μM)	$hNa_V1.5$[b] IC_{50} (μM)	Pred. HLM / RLM CL_{int} (μL/min/mg)[c]	HLM / RLM CL_{int} (μL/min/mg)	LipE[d]
25	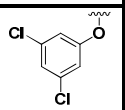	0.036	6.0	13 / 14	< 14 / < 14	5.26
26	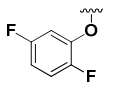	0.100	23.7	15 / 27	< 14 / 33	5.99
27	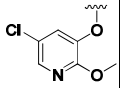	0.150	11.6	15 / 16	< 14 / < 14	6.12
28	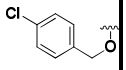	0.109	21	14 / 14	< 14 / < 14	5.36
29		0.20	9.3	18 / 15	< 14 / < 14	5.61
30		0.55	17.8	95 / 14	102 / 17	5.68

31		0.16	8.9	205 / 15	199 / < 14	4.5
32		0.088	2.5	393 / 33	385 / 40	5.77

[a] hNav1.7 data were collected using a PatchXpress automated electrophysiology platform using a protocol where cells were held at a voltage yielding 20-50% channel inactivation. [b] hNav1.5 data were collected on the same platform using a protocol where cells were held at -50 mV. [c] Empirical statistical in silico model derived using the Cubist statistical method and a pool of 820 molecular descriptors. [d] LipE was calculated using hNa$_V$1.7 PX IC_{50} and Amgen Na$_V$1.7 project cLogD(7.4), which was calculated using daylight cLogP and an Amgen pK_a calculator.

With the potent and relatively low clearance 3,5-dichlorophenyl ether tail group in place, replacement of the pyridyl ring Cl with CF_3 was found to afford approximately equivalent potency with a slight loss in selectivity and efficiency (**33**, Table 6). More polar substituents such as CHF_2 (**34**) and CN (**35**) were fairly well tolerated and afforded selective, efficient leads. While compound **35** proved most efficient in this series, the PSA (118) and rat clearance (CL = 1.8 L/h/kg) were high relative to the more potent lead **25** (PSA = 95; rat IV CL = 0.734 L/h/kg). While both compounds were highly bound in rat plasma (rat PPB > 99.9 % bound), the clearance was lower for the less polar lead **25**. Since the chloro-pyridyl middle ring afforded a good balance of favorable properties, it was retained for further optimization.

Table 6. Selected middle ring Cl replacement SAR

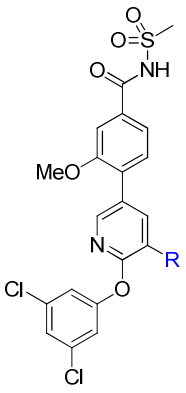

Cmpd	-R	$hNa_V1.7$[a] IC_{50} (μM)	$hNa_V1.5$[b] IC_{50} (μM)	Pred. HLM / RLM CL_{int} (μL/min/mg)[c]	HLM / RLM CL_{int} (μL/min/mg)	LipE[d]
25	Cl	0.036	6.0	13 / 14	< 14 / < 14	5.26
33	CF_3	0.028	2.35	14 / 14	< 14 / < 14	4.97
34	CHF_2	0.054	18.8	18 / 15	< 14 / < 14	5.41
35	CN	0.077	16.1	28 / 15	39 / 15	5.75

[a] hNav1.7 data were collected using a PatchXpress automated electrophysiology platform using a protocol where cells were held at a voltage yielding 20-50% channel inactivation. [b] hNav1.5 data were collected on the same platform using a protocol where cells were held at -50 mV. [c] Empirical statistical in silico model derived using the Cubist statistical method and a pool of 820 molecular descriptors. [d] LipE was calculated using $hNa_V1.7$ PX IC_{50} and Amgen $Na_V1.7$ project cLogD(7.4), which was calculated using daylight cLogP and an Amgen pK_a calculator.

We then returned to weaker ($Na_v1.7$ IC_{50} > 0.075 μM), efficient leads identified in the library exploration described in Table 5 that incorporated relatively small bottom rings, as we imagined that a boost in potency and/or intrinsic stability could be gained via re-introduction of fluorine at C-2 in the top ring. Indeed, this afforded improved potency, selectivity and LipE (**36,** AM-0358[19] vs. **26**; **37** vs. **29**; **38** vs. **30**) as well as improved RLM CL_{int} for **36**. Selected lipophilic efficient leads, incorporating F at C-2, are represented in Table 7.

Table 7. Selected leads incorporating F at C-2

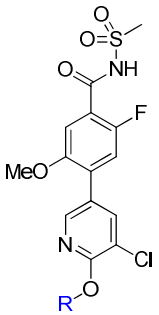

Cmpd	-OR	$hNa_V1.7$[a] IC_{50} (μM)	$hNa_V1.5$[b] IC_{50} (μM)	Pred. HLM / RLM CL_{int} (μL/min/mg)[c]	HLM / RLM CL_{int} (μL/min/mg)	LipE[d]	LE
36	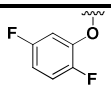	0.069	6.9	20 / < 14	27 / < 14	6.37	0.31
37		0.062	11	93 / < 14	110 / < 14	6.35	0.34
38		0.110	18	124 / < 14	161 / < 14	6.60	0.35

[a] hNav1.7 data were collected using a PatchXpress automated electrophysiology platform using a protocol where cells were held at a voltage yielding 20-50% channel inactivation. [b] hNav1.5 data were collected on the same platform using a protocol where cells were held at -50 mV. [c] Empirical statistical in silico model derived using the Cubist statistical method and a pool of 820 molecular descriptors. [d] Amgen $Na_V1.7$ project cLogD(7.4) was calculated using daylight cLogP and an Amgen pK_a calculator.

As compounds **37** and **38** suffered from high CL_{int} in HLM, they were not advanced. In accordance with its low CL_{int} in RLM, aryl-ether acyl sulfonamide **36** demonstrated low-moderate clearance (CL = 0.39 L/h/kg), as well as high oral bioavailability (F > 100%) and high plasma protein binding (99.6% bound) in rats (Table 8). Based on experimental data suggesting that the reported acyl sulfonamides are substrates for breast cancer resistance protein (BCRP; ABCG2), the high oral bioavailability observed in rats is most likely attributable to a combination of low clearance, high passive permeability (Papp Avg. MDCK: 22.4 μcm/s), high solubility (PBS, FaSSIF: 398, 500 μM), and presumed saturation of rBCRP (hPgp ER 1.4; hBCRP ER 23.7; rBCRP ER 25.7) and/or OATP in the intestine or liver. Further supporting the potential for transporter saturation is the expected intestinal concentration of approximately 454 μM based on a molar dose of 5.1 μmol (10 mg/kg, 0.25 kg rat, MW = 486.9) and an intestinal volume of 11.3 mL.[20] In general, in vitro ADME assays under-predicted the clearance for these

compounds, as is often the case when transporter-mediated clearance pathways are suspected.[21] It is also possible that the observed volume of distribution for **36** is partially a function of hepatobiliary uptake into hepatocyte, as is often the case for acidic compounds.[22] In addition to its favorable rat PK profile, **36** demonstrated no appreciable in vitro time-dependent inhibition of hCYP3A4, 2D6 and 2C9 at concentrations up to 45 μM (Table 9).

Table 8. Rat PK of **36**[a]

Route (mg/kg)	AUC_{inf} (μM-h)	CL (L/h/kg)	$T_{1/2}$ (h)	Vd (L/kg)	F (%)	Plasma Protein Binding (%)
i.v. (1)[b]	5.4 ± 1.2	0.39 ± 0.08	1.84 ± 0.21	0.93 ± 0.19	--	99.6 ± 0.01
p.o. (10)[c]	377 ± 44.2	--	--	--	>100	

[a] Male, Fed. [b] Vehicle: 100% DMSO. [c] Vehicle: 1%Tween 80, 2%HPMC, 97% water/NaOH(pH 8.5).

Table 9. hCYP Inhibitory activity of **36**

hCYP	3A4	2D6	2C9
IC_{50} (μM)[a]	>50	>50	45.3
Shifted IC_{50} (μM)[b]	>50	>50	49.6

[a] Compound **36** was co-incubated with probe substrate of enzyme activity. [b] Compound **36** was pre-incubated with enzyme and co-factor for 30 minutes prior to addition of probe substrate to determine potential for time-dependent inhibition.

While **36** was not a potent inhibitor of rat $Na_V1.7$ heterologously expressed in HEK cells (IC_{50} = 3.69 μM), its potency on mouse $Na_V1.7$ (IC_{50} = 0.115 μM) was comparable to that observed on the human channel, and it potently inhibited native TTX-S currents in mouse DRG neurons, with IC_{50} = 0.27 μM.

Consequently, the pharmacokinetic-pharmacodynamic (PK-PD) behavior of **36** was evaluated in a mouse histamine-induced scratching model (Figure 1, A), which we have shown to be $Na_V1.7$

dependent.[4c] The importance of $Na_V1.7$ in itch pathways has also been established in humans,[7] and we anticipate a potential utility of itch as a biomarker in human clinical trials. With an oral dose of 300 mg/kg, **36** demonstrated robust reduction of histamine-induced scratching bouts (75%, which was comparable to the anti-histamine control, diphenhydramine, at 30 mg/kg) with unbound plasma concentrations (mPPB = 98.6%, Cu plasma = 4.15 μM) ~15-fold greater than the IC_{50} as measured on native TTX-S currents in mouse DRG neurons. Notably, the same oral dose and similar plasma exposure was not associated with any significant reductions in activity in a separate open-field study in naïve mice (Figure 1, B). At lower doses (30, 100 mg/kg), the effect on histamine-induced scratching bouts was not statistically significant. The steep dose-response and the requirement for relatively high target coverage (~15-fold vs. mouse DRG IC_{50}) in this model are in line with the PK-PD relationship spanning a substantial internal data set of related compounds. Furthermore, this is consistent with published coverage multiples in rodent PD assays from an aryl sulfonamide compound which ranged from 10x to 330x. [10a] Also consistent with these findings, inhibition of a large fraction of Nav current is required to block action potential firing in neurons.[23]

Figure 1. Dose response of compound **36** in mice: (A) Histamine-Induced Scratching; (B) Open Field Assessment (PK/PD)[a]

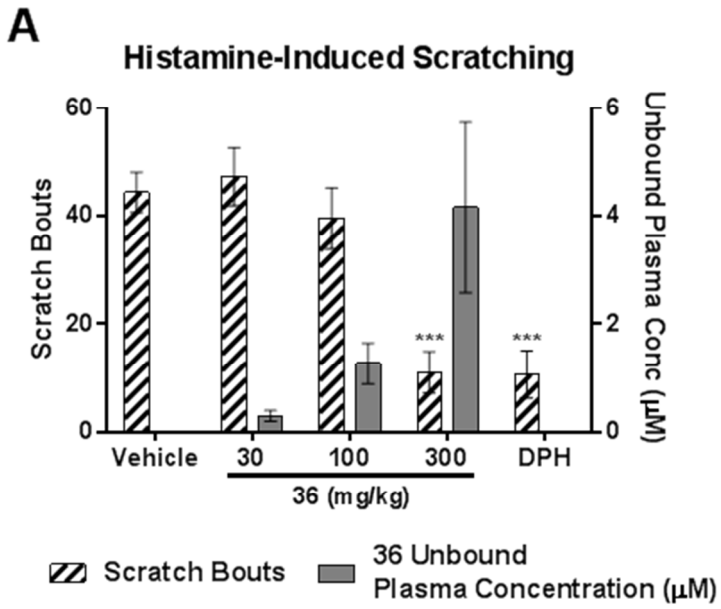

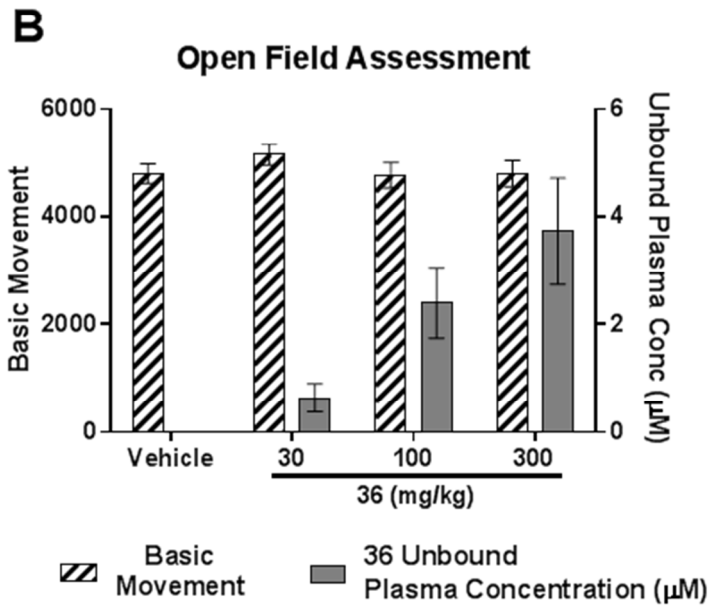

Dose (mg/kg)		30	100	300
mean Plasma Cu (μM)	A. HIS	0.294 ± 0.099	1.27 ± 0.379	4.16 ± 1.58
	B. Open Field	0.640 ± 0.250	2.39 ± 0.650	3.72 ± 0.990

[a] **A: Mouse Histamine-Induced Scratching –** Total number of histamine-induced scratch bouts in animal cohorts orally administered either vehicle (veh, n =12), diphenhydramine (DPH, 30 mg/kg, n = 8), or 30 (n = 9), 100 (n = 10), or 300 (n = 10) mg/kg of **36**. All treatment groups received histamine i.d. ***, $p < 0.001$ versus vehicle group (one-way ANOVA followed by Dunnett's test). **B: Mouse Open Field Assessment –** Total basic movement in an open-field arena recorded following oral administration of either vehicle (veh, n = 10) or **36** at 30, 100, or 300 mg/kg (n = 10 for each dose).

Compound **36** was evaluated, via manual patch clamp electrophysiology, for inhibitory activity against a panel of other human sodium channel isoforms, where it demonstrated marked selectivity (Table 10). Furthermore, **36** was highly selective over other important anti-targets such as hERG (K_i > 30 μM), hCYPs (Table 9), and hBSEP (IC_{50} = 13.3 μM).[24] Notably, selectivity over hCYP2C9 is substantially enhanced relative to reported heteroaryl sulfonamide $hNa_V1.7$ inhibitors.[10] Furthermore, no significant induction of hPXR was observed at concentrations 200-fold in excess of the $hNa_V1.7$ IC_{50} (3.2 % at 2 μM, 3.2 % at 10 μM).

Table 10. Manual E-phys – Inhibitory activity of **36** across the human Na_V family panel[a]

$hNa_V1.x$	1.7	1.1	1.2	1.3	1.4	1.5	1.6	1.8
IC_{50} (μM)	0.051 ± 0.012	8.5 ± 2.26	9.8 ± 3.7	12.5 ± 3.9	1.1 ± 0.32	11.9 ± 2.2	9.4 ± 0.46	15.6 ± 0.49

[a] Values represent the mean of two experiments. Data were collected by manual patch clamp electrophysiology using a protocol where cells were held at a voltage yielding 20% channel inactivation.

In order to measure use-dependence of channel inhibition, a representative set of compounds was evaluated for inhibitory activity on hNav1.7 and hNav1.5 using an IonWorks Quattro (IWQ) automated electrophysiology system. The protocol allowed for IC_{50} measurements at pulse 1 (tonic block) and pulse 26 (use-dependent block) (See SI, Table S4). In general, the biaryl acyl sulfonamides are not use-dependent inhibitors of these channels. For example, compound **36**: Nav1.7 IWQ IC_{50} tonic = 0.044 μM, IC_{50} use = 0.042 μM; Nav1.5 IWQ IC_{50} tonic = 13.6 μM,

IC_{50} use = 11.4 μM). In order to measure state-dependence, compound **36** was evaluated on hNav1.7 using manual patch clamp electrophysiology. In this experiment, we measured inhibitory activity on the channels in the resting/closed state (V-hold = -140 mV) and a partially inactivated state (initial V-hold = -140 mV, then switch to a voltage that yielded ~ 20% channel inactivation). The data set indicates that the inhibition of hNav1.7 by **36** is state-dependent (mean IC_{50} on resting/closed channels >30 μM (n = 3 cells); mean IC_{50} on ~20% inactivated channels = 0.051 μM (n = 2 cells)).

In a hNav1.7 radioligand binding assay using a tritiated ligand that was derived from our internal optimization of 6,6-fused aryl heteroaryl sulfonamide leads such as **3**,[25] acyl sulfonamide **36** potently displaced the labeled heteroaryl sulfonamide with IC_{50} = 0.017 μM. This data, in combination with parallel SAR from the two series, including markedly decreased potency on rat $Na_V1.7$, suggests that our heteroaryl sulfonamides and acyl sulfonamides occupy the same binding pocket in $Na_V1.7$, as initially assumed. **36** was docked into the known binding pocket of GX-936 in the $Na_V1.7$ VSD4 region, using the recently disclosed co-crystal structure (Figure 2).[26] The presumed binding mode of **36** is in agreement with the observed SAR and biological activity. With this docked model, we hypothesize that the SO_2 group of **36** aligns with the thiadiazole group of GX-936, to interact with R1608, while the CO group of **36** aligns with the SO_2 group of GX-936 to interact with R1602 and R1605. The model also suggests that the top ring C-5 methoxy substituent of **36** aligns with the CN substituent of GX-936, projecting towards polar D1586, thus explaining tolerance for small polar substituents at this position (e.g., OMe, CN). In contrast, the top ring C-3 of **36** faces a lipophilic wall, consistent with the observed intolerance for substitution larger than fluorine or replacement with pyridyl (N). The docked model aligns the pyridyl ring C-3 Cl with the positively charged azetidine ring of GX-936,

projecting towards polar residue E1534, supporting the observed tolerance for small polar substituents (e.g., CHF_2, CN) at this position. As was observed with GX-936, the model predicts that the top ring of **36** forms a π-stacking interaction with Y1537, while the terminal 2,5-difluorophenyl ring forms a unique π-stacking interaction with W1538. Based on sequence alignment between $Na_V1.7$ and $Na_V1.5$, the residues in the positions of Y1537 and W1538 in hNav1.5 are alanine and lysine, respectively. According to this model, the inability of biaryl acyl sulfonamides to form π-stacking interactions with these residues in $Na_V1.5$ likely contributes to the observed selectivity.

Figure 2. **36** docked into VSD4 of chimeric $Na_V1.7$[a]

A.

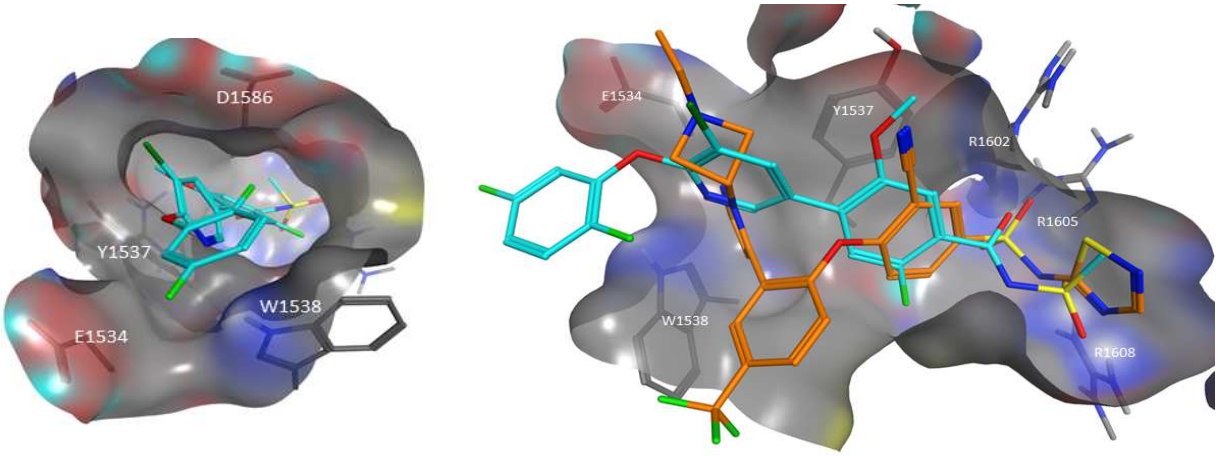

B.

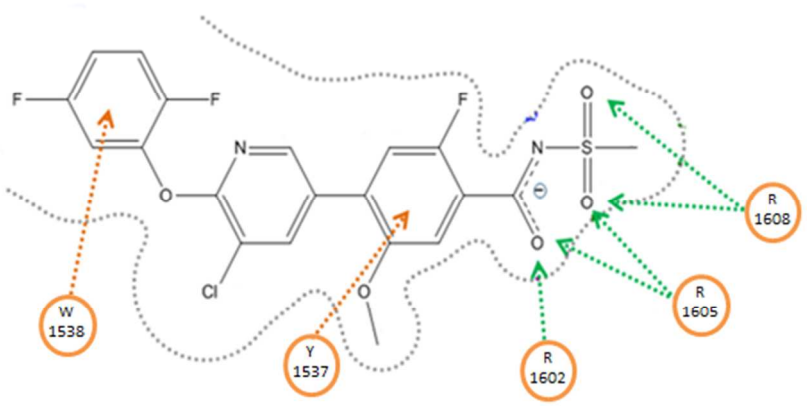

[a] All displayed AA residues are within 4.5 Å of compound **36** in the binding surface model. **A**. Docked conformation of **36** (blue) superimposed onto the experimental coordinates of the GX-936 (orange)-VSD4-Na_VAb crystal structure as viewed from two angles. **B. 36**-protein interaction map. Orange: π-stacking or hydrophobic interaction; Green: polar or charge-charge interaction.

CHEMISTRY

Scheme 3 describes the synthesis of isoquinoline thiadiazole sulfonamide **3** and isoquinoline acyl sulfonamides **4-6**. Palladium catalyzed coupling of 6-bromo-1-chloroisoquinoline **39** and phenylmethanethiol afforded benzylmercaptan **40**. **40** was converted to **41** via oxidation with 1,3-dichloro-5,5-dimethylimidazolidine-2,4-dione followed by condensation with 2,3,4,5,6-pentafluorophenol. Reaction with *N*-(2,4-dimethoxybenzyl)-1,2,4-thiadiazol-5-amine in the presence of LiHMDS afforded **42**, which was converted to **3** via Suzuki coupling to (3-chloro-4-(trifluoromethyl)phenyl)boronic acid. 1-Chloroisoquinoline-6-carboxylic acid **43** was subjected to Suzuki coupling with (3-chloro-4-(trifluoromethyl)phenyl)boronic acid to afford **44**, which was then condensed with methanesulfonamide in the presence of EDC to afford **4.** Alternatively, EDC-promoted coupling of methanesulfonamide and **43** afforded **45**. S_NAr of **45** with 4-chloro-3-(trifluoromethyl)phenol or **48** afforded **5** and **6**, respectively. Phenol **48** was derived from

bromide **46** via S_NAr with 2-methylpropan-1-ol to give intermediate **47**, followed by borylation and oxidation.

Scheme 3. Preparation of Compounds **3, 4, 5**, and **6**[a]

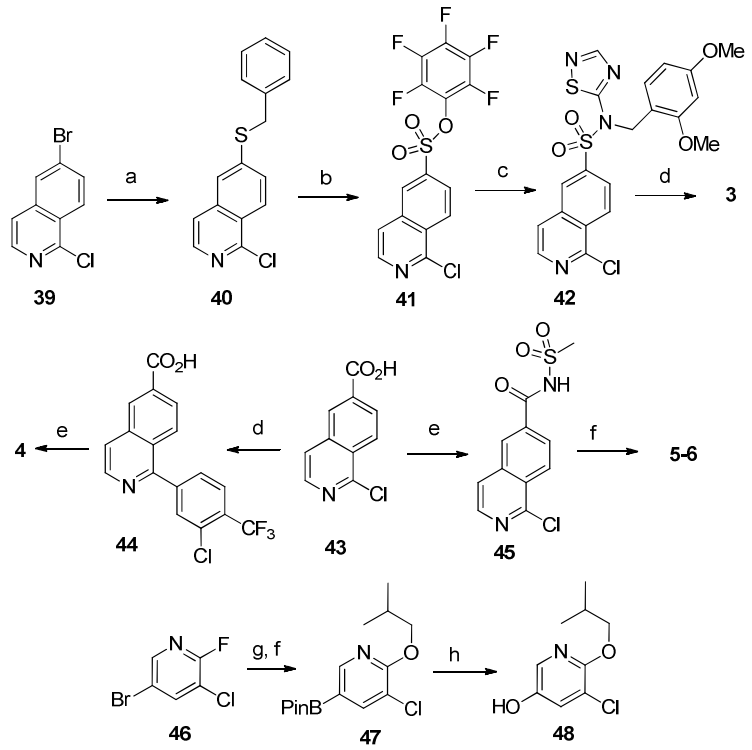

[a] Reagents and conditions: (a) Xantphos, $Pd_2(dba)_3$, DIPEA, phenylmethanethiol, 1,4-dioxane (63%); (b) i. 1,3-dichloro-5,5-dimethylimidazolidine-2,4-dione, CH_3CN, water, AcOH, 0 °C; ii. 2,3,4,5,6-pentafluorophenol, CH_3CN (74%); (c) *N*-(2,4-dimethoxybenzyl)-1,2,4-thiadiazol-5-amine, LiHMDS, THF (83%); (d) (3-chloro-4-(trifluoromethyl)phenyl)boronic acid, $Pd(PPh_3)_4$, K_2CO_3, 1,4-dioxane/water, 100 °C (14-66%); (e) NH_2SO_2Me, EDC-HCl, DMAP, DCM (47-60%); (f) 4-chloro-3-(trifluoromethyl)phenol (for **5**) or **48** (for **6**) or 2-methylpropan-1-ol (for **47**), Cs_2CO_3, DMSO, 90 °C (37-86%); (g) bis(pinacolato)diboron, $PdCl_2(dppf)\cdot DCM$, KOAc, 1,4-dioxane, 90 °C (47%); (h) oxone, acetone/water, 0 °C (65%).

Scheme 4 demonstrates synthetic routes to biaryl acyl sulfonamides **8-9**, **11-18**, **20-33** and **36-38**. 4-Bromo-2-fluoro-5-methoxybenzoic acid **51a** was prepared from **49**, following a sequence of saponification and bromination to provide intermediate **50**, followed by per-methylation and saponification. **51b-p** were obtained from commercial suppliers. Aryl bromides **52a-p** were prepared from EDC-promoted coupling of carboxylic acids **51a-p**. Suzuki coupling of **52a-p**

with either commercial boronates or **47** afforded final compounds **8-9** and **11-18**, and intermediates **24** and **53-54**. Fluoride **24**, prepared from 4-bromo-3-methoxy-N-(methylsulfonyl)benzamide (**52p**), was reacted with alcohols under parallel S_NAr conditions to afford ether-linked final compounds **25-30**. In a similar fashion, **33** was prepared from fluoride **53** and **36-38** were prepared from fluoride **54**. Similarly, base-promoted S_NAr reactions of thiols or amines with fluoride **24** afforded compounds such as **31** and **32**.

Scheme 4. Preparation of Compounds **8-9**, **11-18**, **20-33** and **36-38**[a]

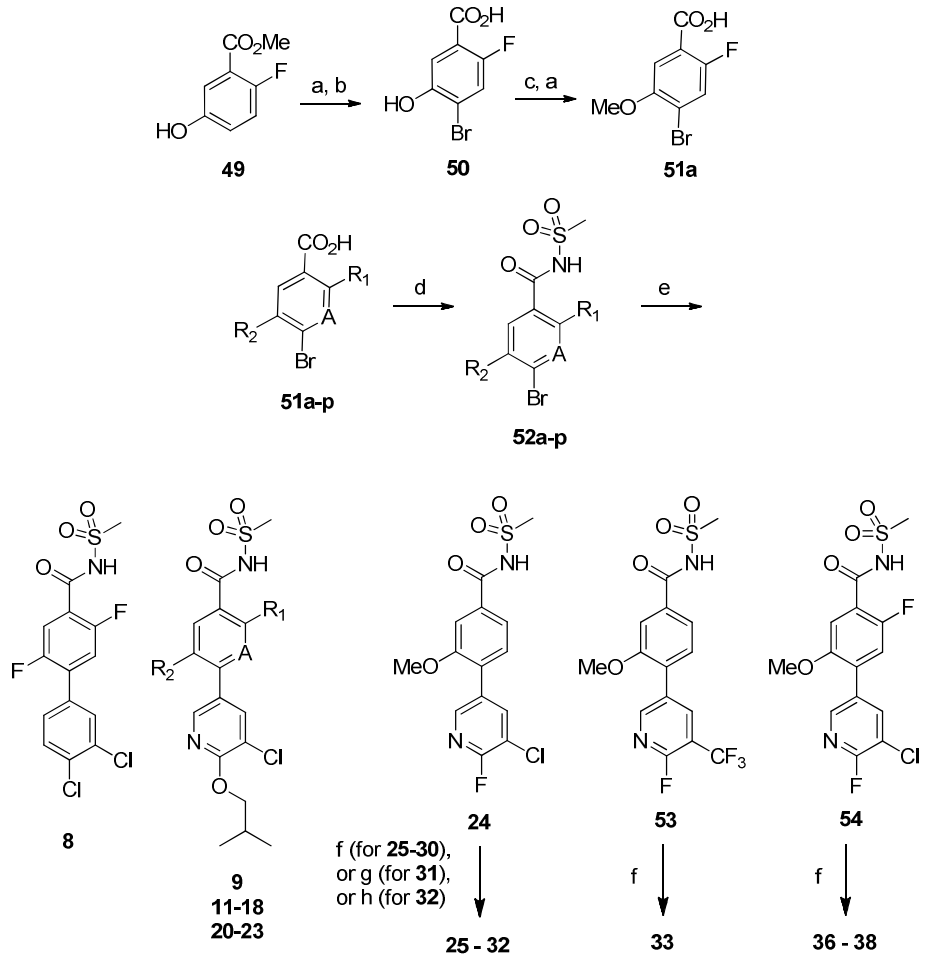

[a] Reagents and conditions: (a) LiOH, water/THF, RT (91-94%); (b) Br_2, AcOH, DCM, RT (47%); (c) Me_2SO_4, K_2CO_3, CH_3CN, 80 °C (38%); (d) NH_2SO_2Me, EDC-HCl, DMAP, DCM, RT (81-92%); (e) aryl boronate, $Pd(PPh_3)_4$, K_2CO_3 (or Na_2CO_3), 1,4-dioxane/water, 60 °C (or reflux) (37-91%); (f) alcohol, Cs_2CO_3, DMSO, 90 - 120 °C (18-79%); (g) 3-

methylbenzenethiol, Cs_2CO_3, DMSO, 100 °C (26%); (h) i. 2-isopropylpyrrolidine, NEt_3, DMSO, 90 °C (68%); ii. SFC with Chiralpak-IC.

The synthesis of compounds **10** and **19** is described in Scheme 5. Carboxylic acids **55** and **57** were converted into the corresponding acyl sulfonamides, which were then coupled under Suzuki conditions to 5-bromo-3-chloro-2-isobutoxypyridine or 3-chloro-2-isobutoxypyridine-5-boronic acid, respectively, affording compound **10** and intermediate **59**. Suzuki coupling of bromide **59** to 2-(2,5-dihydrofuran-3-yl)-4,4,5,5-tetramethyl-1,3,2-dioxaborolane afforded compound **19**.

Scheme 5. Preparation of Compounds **10** and **19**[a]

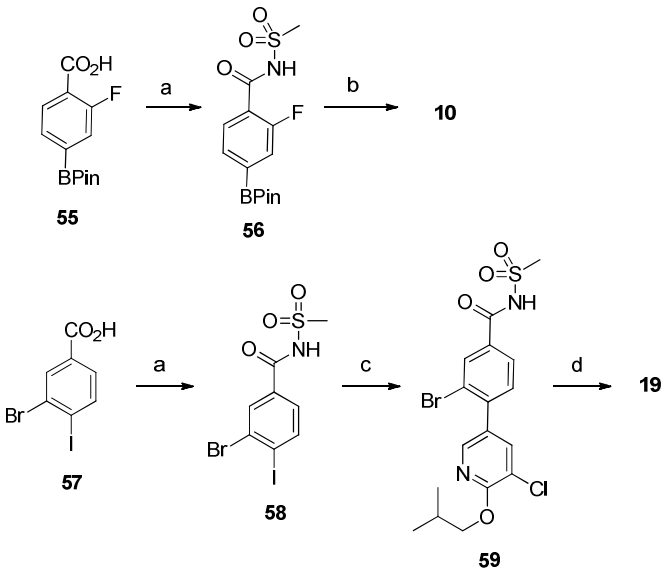

[a] Reagents and conditions: (b) NH_2SO_2Me, EDC-HCl, DMAP, DCM, RT (34-43%); (b) 5-bromo-3-chloro-2-isobutoxypyridine, $Pd(PPh_3)_4$, K_2CO_3, 1,4-dioxane/water, 60 °C (44%); (c) 3-chloro-2-isobutoxypyridine-5-boronic acid, $PdCl_2(dppf)\cdot DCM$, $Pd_2(dba)_3$, K_2CO_3, 1,4-dioxane/water, *t*-BuOH, 50 °C (49%); (d) 2-(2,5-dihydrofuran-3-yl)-4,4,5,5-tetramethyl-1,3,2-dioxaborolane, $PdCl_2(dppf)\cdot DCM$, $Pd_2(dba)_3$, K_2CO_3, 1,4-dioxane/water, *t*-BuOH, 95 °C (12%).

The synthesis of compounds **34** and **35** is described in Scheme 6. S_NAr of fluoro-pyridyl boronic ester **60** with 3,5-dichlorophenol afforded boronate **61**, which was coupled to **52p** to generate aldehyde **62**. Reaction of **62** with DAST afforded difluoromethyl compound **34**. Boronate **64** was prepared from bromide **63** and coupled to **52p** to generate aniline **65**.

Sandmeyer reaction with CuBr afforded bromide **66**, which was converted to nitrile **67** by microwave-promoted palladium-catalyzed coupling to $Zn(CN)_2$. S_NAr reaction with 3,5-dichlorophenol afforded final compound **35**.

Scheme 6. Preparation of Compounds **34** and **35**[a]

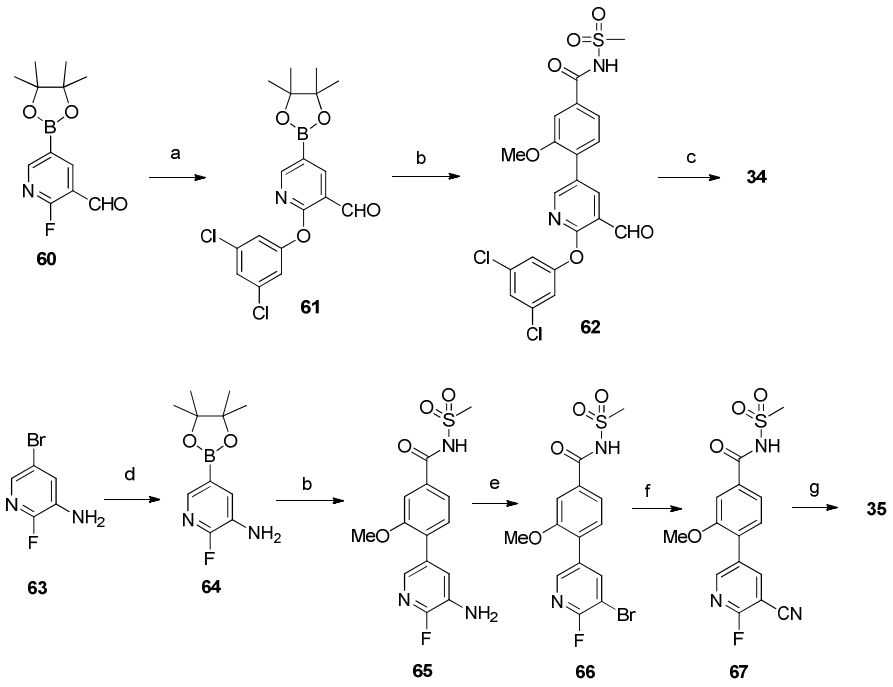

[a] Reagents and conditions: (a) 3,5-dichlorophenol, Cs_2CO_3, DMF, 50 °C (26%); (b) **52p**, $Pd(PPh_3)_4$, K_2CO_3 (or Na_2CO_3), 1,4-dioxane/water 90 °C (42-46%); (c) DAST, DCM 50 °C (8%); (d) bis(pinacolato)diboron, $PdCl_2(dppf)$·DCM, KOAc, 1,4-dioxane, 90 °C (84%); (e) isoamylnitrite, CuBr, CH_3CN (40%); (f) $Zn(CN)_2$, $Pd_2(dba)_3$, XantPhos, DMF, 100 °C, μW (63%); (g) 3,5-dichlorophenol, Cs_2CO_3, DMSO, 90 °C (80%).

CONCLUSION

Parallel synthetic strategies, with focus on molecular weight and lipophilicity, were applied in the rapid generation of potent, selective, and efficient leads in a novel class of biaryl acyl sulfonamide $Na_V1.7$ inhibitors. Representative lead **36** demonstrated marked selectivity against seven other hNa_V isoforms, hERG, hCYPs, hPXR, and hBSEP. Its good rodent pharmacokinetics and robust pharmacodynamic response in a mouse histamine-induced

scratching model (without associated locomotor side effects) are typical of this series of compounds. As such, leads from this series are anticipated to be quality tools for probing the target coverage requirements for efficacy in various preclinical rodent models of acute and chronic pain. Furthermore, compound **36** and related leads described herein compare favorably to reported heteroaryl sulfonamides with respect to their lack of CYP inhibition. While the current leads in this biaryl acyl sulfonamides series would benefit from further gains in potency without compromising PK, thus affording lower efficacious doses, the low probability of drug-drug interactions with future derived compounds is noteworthy. Moreover, the modular nature of the scaffold and modeling in the $Na_V1.7$ VSD4 selectivity pocket should enable rapid lead optimization. Related efforts will be reported in due course.

EXPERIMENTAL SECTION

Unless otherwise noted, all materials were obtained from commercial suppliers and used without further purification. Anhydrous solvents were obtained from Aldrich and used directly. All reactions involving air- or moisture–sensitive reagents were performed under a nitrogen or argon atmosphere. Microwave-assisted reactions were conducted with a Biotage Initiator. Purifications were performed using standard column chromatography in glass columns or medium pressure liquid chromatography (MPLC) on a CombiFlash Companion (Teledyne Isco) or a Biotage Isolera with prepacked RediSep or Biotage normal-phase silica gel (35−60 μm) columns and UV detection at 254 nm. Preparative reversed-phase high-performance liquid chromatography (HPLC) and high throughput parallel purification were performed with reversed phase preparative LC/MS: Waters auto-purification system; liquid transfer system: Tecan; drying system: Genevac; prep. Column: Xbridge (19 x 100 mm, C18, 10 μm); flow rate: 40 mL/min; general gradient: 5 – 95% B, 0.1% additive in both A and B; 10 min gradient; Mobile Phase A:

H_2O, Mobile Phase B, CH_3CN; Additive: TFA or NH_4OH. Chiral method development was performed on an analytical Thar SFC/MS. Preparative chiral separations were performed on Thar SFC Prep 80 or SFC Prep 350 instruments. All final compounds were purified to ≥ 95% purity as determined by HPLC. Purity (3 min methods only) and reaction analyses were measured using Agilent 1100 Series HPLC systems with UV detection at 254 nm and 215 nm (System A: Agilent Zorbax SB-C18 3.0 x 50 mm, 3.5 micron, 5 to 95% CH_3CN in H_2O with 0.1% TFA for 3.6 min at 1.5 mL/min or Halo Phenyl-Hexyl, 3 x 50 mm, 2.7 micron, 5 to 95% CH_3CN in H_2O with 0.1% TFA for 1.01 min at 2.0 mL/min; System B: Waters Xbridge C18, 3 x 50 mm, 3.5 micron, 5 to 95% CH_3CN in H_2O with 0.1% formic acid for 3.6 min at 1.5 mL/min. ^1H NMR spectra were recorded at ambient temperature on a Bruker AV-400 (400 MHz) spectrometer or a Varian 400 MHz spectrometer or a Bruker Advance III spectrometer, operating at a proton frequency of 500.34 MHz using a Protasis CapNMR flow-probe, equipped with Discovery Tower™ Sample management system and a Waters Liquid Handler, made by CTC, Switzerland (Model 2777). All observed protons are reported as parts per million (ppm) downfield from tetramethylsilane (TMS) or other internal reference in the appropriate solvent indicated. Data are reported as follows: chemical shift, multiplicity (s = singlet, d = doublet, t = triplet, q = quartet, br = broad, m = multiplet), coupling constants, and number of protons. Low-resolution mass spectral (MS) data were determined on an Agilent 1100 Series LCMS with UV detection at 254 nm and a low resonance electrospray mode (ESI). Exact mass confirmation was performed on an Agilent 1200 series high performance liquid chromatography (HPLC) system (Santa Clara, S2 CA, U.S.) by flow injection analysis, eluting with a binary solvent system A and B (A, water with 0.1% formic acid; B, CH_3CN with 0.1% formic acid) under gradient conditions (5-95% B

over 3 min) at 0.3 mL/min with MS detection by an Agilent 6510-Q-TOF mass spectrometer (Santa Clara, CA, U.S.).

1-(3-Chloro-4-(trifluoromethyl)phenyl)-*N*-1,2,4-thiadiazol-5-yl-6-isoquinolinesulfonamide (3). Step 1A. To a suspension of 1,2,4-thiadiazol-5-amine (3.35 g, 33.1 mmol) and 2,4-dimethoxybenzaldehyde (5 g, 30.1 mmol) in DCM (150 mL) was added chlorotitanium triisopropoxide (19.60 g, 75 mmol) in DCM (10 mL) portion wise over 5 min. After stirring for 15 min, sodium triacetoxyborohydride (31.9 g, 150 mmol) was added portionwise and the reaction mixture was stirred for 1 h and quenched with saturated aq. $NaHCO_3$ to pH~7, added 50 mL of water to aid layer separation. The mixture was then extracted with DCM (3 x 100 mL). The combined organics were dried over $MgSO_4$, filtered, and concentrated to afford a yellow residue, which was purified by column chromatography using isocratic Hex:EtOAc (50:50) to obtain *N*-(2,4-dimethoxybenzyl)-1,2,4-thiadiazol-5-amine (3 g, 11.94 mmol, 39.7 % yield) as an off-white solid. Step 1B. A 3 neck 2L flask equipped with overhead stirrer, thermocouple and nitrogen inlet was charged with 6-bromo-1-chloroisoquinoline **39** (60 g, 247 mmol), Xantphos (7.16 g, 12.37 mmol) and $Pd_2(dba)_3$ (5.66 g, 6.19 mmol). To reaction flask was charged with 1,4-dioxane (540 mL) and DIPEA (64.8 mL, 371 mmol). The flask was purged with N_2 and heated to 63 °C upon which a solution of phenylmethanethiol (30.5 mL, 260 mmol) in 180 mL of sparged 1,4-dioxane was charged to the reaction mixture dropwise over 1 h. The reaction mixture was filtered and concentrated to obtain an oil. Upon charging 500 mL isopropanol to the oil, a crystalline slurry was formed. This was stirred at RT for 2 h, cooled to 0 °C and filtered. The solids were washed with 50% IPA/heptane, then dried under vacuum with a nitrogen sweep to obtain 6-(benzylthio)-1-chloroisoquinoline **40** (44.3 g, 63% yield) as a yellow solid. MS (ESI, positive ion) m/z: 286.0 $[M+1]^+$. Step 2B: A 3 neck 2000 mL flask equipped with overhead

stirrer, thermocouple and nitrogen inlet was charged with **40** (35.8 g, 125 mmol), CH_3CN (360 mL), water (29.5 mL) and AcOH (44.6 mL). The resulting mixture was cooled to 0-5°C upon which 1,3-dichloro-5,5-dimethylimidazolidine-2,4-dione (49.4 g, 251 mmol) was charged as a solid portionwise, maintaining the temperature < 10 °C. 2,3,4,5,6-Pentafluorophenol (45 g, 244 mmol) was charged to the reaction as a solution in 45 mL CH_3CN then charged triethylamine (48.0 mL, 344 mmol) dropwise via syringe over 2 h. Water (250 mL) was charged to the reaction. The product crystallized out of solution and was filtered and washed with water. Upon drying overnight under vacuum with a nitrogen sweep, perfluorophenyl 1-chloroisoquinoline-6-sulfonate **41** (38.14 g, 74% yield) was obtained as off white amorphous solid. MS (ESI, positive ion) m/z: 409.9 $[M+1]^+$. Step 1C. A 3 neck flask equipped with magnetic stirrer, thermocouple and nitrogen inlet was charged with **41** (6.5 g, 15.86 mmol), *N*-(2,4-dimethoxybenzyl)-1,2,4-thiadiazol-5-amine (4.39 g, 17.45 mmol) and THF (70 mL). The solution was cooled to 0 °C and LiHMDS (19.04 mL, 19.04 mmol) was charged dropwise via syringe. The reaction mixture was stirred for 30 min and reverse quenched into DCM and 1N HCl. The organic layer was separated and dried over sodium sulfate and concentrated. MTBE/IPA was charged to resulting yellow solids and stirred for 1 h. The solid was filtered and washed with MTBE and dried under vacuum with a nitrogen sweep to afford 1-chloro-N-(2,4-dimethoxybenzyl)-*N*-(1,2,4-thiadiazol-5-yl)isoquinoline-6-sulfonamide **42** (6.28 g, 83%) as pale yellow solid. MS (ESI, positive ion) m/z: 477.0 $[M+1]^+$. Step 2C. A vial was charged with **42** (0.08 g, 0.17 mmol), potassium carbonate (0.12 g, 0.84 mmol), (3-chloro-4-(trifluoromethyl)phenyl)boronic acid (0.05 g, 0.20 mmol) and $Pd(PPh_3)_4$ (0.02 g, 0.02 mmol) in 1,4-dioxane (1.1 mL) and water (0.6 mL) and heated at 100 °C for 30 min, while shaking on a J-KEM block. The reaction mixture was filtered through a celite plug and purified by reversed

phase preparative LC/MS: Column: Xbridge (19 x 100 mm, C18, 10 μm); flow rate: 40 mL/min; 10 min gradient 5 – 95% CH_3CN / 0.1% NH_4OH in H_2O to afford the title compound (8.7 mg, 14% yield) as a white solid. MS (ESI, positive ion) m/z: 471.0 $[M+1]^+$. ^1H NMR (400MHz, DMSO-d_6) δ 8.73-8.79 (m, 1H), 8.62-8.66 (m, 1H), 8.45-8.50 (m, 1H), 8.11-8.23 (m, 3H), 8.00-8.06 (m, 1H), 7.88-7.99 (m, 2H). ^{13}C NMR (126 MHz, DMSO-d6) δ 177.2, 160.2, 156.6, 142.5, 141.8, 141.0, 135.6, 133.4, 133.0, 132.8, 131.3, 128.6, 128.1, 128.0, 126.5, 125.9, 123.5, 121.6. HRMS m/z: Calcd for $C_{18}H_{11}ClF_3N_4O_2S_2$: $[M+1]^+$ = 470.9964. Found $[M+1]^+$ = 470.9959.

1-(3-Chloro-4-(trifluoromethyl)phenyl)-N-(methylsulfonyl)-6-isoquinolinecarboxamide (4). Step 1. A microwave vial was charged with (3-chloro-4-(trifluoromethyl)phenyl)boronic acid (0.11 g, 0.48 mmol), 1-chloroisoquinoline-6-carboxylic acid **43** (0.05 g, 0.24 mmol), $Pd(PPh_3)_4$ (0.03 g, 0.024 mmol), and potassium carbonate (0.10 g, 0.72 mmol). 1,4-dioxane (1.20 ml) and water (0.40 mL) were added and the reaction vial was sealed and irradiated in microwave at 100 ºC for 30 min. The reaction mixture was diluted with ethyl acetate and washed with 1M sodium hydroxide solution, resulting in an emulsion which was acidified with concentrated hydrochloric acid. The aqueous layer was extracted with ethyl acetate and the combined organic layers were dried with sodium sulfate, filtered, and concentrated to afford 1-(3-chloro-4-(trifluoromethyl)phenyl)isoquinoline-6-carboxylic acid **44** (0.06 g, 66 % yield) as a yellow solid. MS (ESI, positive ion) m/z: 352.1 $[M+1]^+$. Step 2. To a solution of **44** (0.06 g, 0.16 mmol) and HBTU (0.09 g, 0.24 mmol) in DMF (0.8 mL) was added DIPEA (0.08 mL, 0.48 mmol) and the mixture was stirred for 16 h at RT. The reaction mixture was purified by Gilson HPLC (25-70% CH_3CN:H_2O w/ /1% TFA modifier). The product fractions were partitioned between ethyl acetate and water and the aqueous layer was extracted with ethyl acetate, and the combined organic layers were dried over sodium sulfate, filtered, and concentrated to obtain the title

compound (0.03 g, 47 % yield) as a white solid. MS (ESI, positive ion) m/z: 429.2 $[M+1]^+$; ^{1}H NMR (400MHz, DMSO-d_6) δ 8.76 (d, J = 5.7 Hz, 1H), 8.74 (d, J = 1.5 Hz, 1H), 8.13 - 8.03 (m, 5H), 7.87 (d, J = 8.7 Hz, 1H), 3.43 (s, 3H). ^{13}C NMR (126 MHz, DMSO-d6) δ 166.0, 156.8, 144.2, 143.0, 135.5, 133.1, 132.5, 131.0, 129.1, 128.9, 128.1, 128.0, 126.9, 126.8, 126.6, 124.0, 122.1, 41.3. HRMS m/z: Calcd for $C_{18}H_{12}ClF_3N_2O_3S$: $[M]^+$ = 428.0209. Found $[M]^+$ = 428.0213.

1-(4-Chloro-3-(trifluoromethyl)phenoxy)-*N*-(methylsulfonyl)-6-isoquinolinecarboxamide (5). STEP 1: A suspension of DMAP (22.74 g, 186 mmol), methanesulfonamide (14.16 g, 149 mmol) and 1-chloroisoquinoline-6-carboxylic acid **43** (25.76 g, 124 mmol) in CH_2Cl_2 (496 mL) was cooled in an ice water bath prior to the addition of EDC·HCl (35.7 g, 186 mmol). The mixture was allowed to slowly warm to RT and stirred overnight at RT. The resulting mixture was concentrated under reduced pressure and purified with MPLC (800 g Interchim HC silica cartridge; solvents: A: DCM, B: 50/50/2.5 methanol/DCM/HCOOH; flow rate: 250 mL/min) to afford 1-chloro-N-(methylsulfonyl)isoquinoline-6-carboxamide **45** (21.3 g, 60.3%). MS (ESI, positive ion) m/z: 285 $[M+1]^+$. ^{1}H NMR (400 MHz, DMSO-d_6) δ 12.50 (br s, 1H), 8.70 (s, 1H), 8.44-8.43 (m, 1H), 8.38-8.35 (m, 1H), 8.21-8.19 (m, 1H), 8.06-8.04 (m, 1H), 3.45 (s, 3H). STEP 2: Using General Procedure A, coupling of **45** and 4-chloro-3-(trifluoromethyl)phenol afforded the title compound (239 mg, 51.2% yield) as a white solid. MS (ESI, positive ion) m/z: 445.3 $[M+1]^+$. ^{1}H NMR (500 MHz, DMSO-d_6) δ 8.55 (s, 1 H), 8.37 (d, J = 8.42 Hz, 1 H), 8.23 (d, J = 9.22 Hz, 1 H), 7.97 (d, J = 5.84 Hz, 1 H), 7.89 (d, J = 2.58 Hz, 1 H), 7.82 (d, J = 8.76 Hz, 1 H), 7.58 - 7.73 (m, 2 H), 3.06 (s, 3 H). ^{13}C NMR (126 MHz, DMSO-d6) δ 166.1, 159.2, 152.0, 140.3, 137.4, 134.1, 132.9, 128.2, 127.9, 126.8, 126.3, 124.2, 123.5, 122.1, 121.3, 120.2, 117.9, 41.3. HRMS m/z: Calcd for $C_{18}H_{12}ClF_3N_2O_4S$: $[M+1]^+$ = 445.0237. Found $[M+1]^+$ = 445.0234.

1-((5-Chloro-6-isobutoxypyridin-3-yl)oxy)-N-(methylsulfonyl)isoquinoline-6-carboxamide (6). STEP 1: To a solution of 5-bromo-3-chloro-2-fluoropyridine **46** (5.00 g, 23.7 mmol) and 2-methylpropan-1-ol (5.28 g, 71.3 mmol) in DMSO (100 mL) was added Cs_2CO_3 (23.0 g, 71.3 mmol) and the reaction was heated at 90 °C for 3 h. The reaction mixture was allowed to cool to RT. H_2O (500 mL) was added and the aqueous layer was extracted with Et_2O (2 x 500 mL). The combined organic extracts were dried over sodium sulfate and concentrated under reduced pressure to obtain the crude material which was purified by column chromatography (silica gel, gradient: 0-5% EtOAc in hexanes) to obtain 5-bromo-3-chloro-2-isobutoxypyridine (5.0 g, 86% yield) as a colorless oil. MS (ESI, positive ion) m/z: no ionization. ^{1}H NMR (400 MHz, $CDCl_3$) δ 8.06 (d, *J* = 2.2 Hz, 1H), 7.74 (d, *J* = 2.2 Hz, 1H), 4.11 (d, *J* = 6.7 Hz, 2H), 2.12 (dt, *J* = 13.4, 6.7 Hz, 1H), 1.03 (d, *J* = 6.7 Hz, 6H). STEP-2: To a solution of 5-bromo-3-chloro-2-isobutoxypyridine (11.0 g, 41.5 mmol) and bis(pinacolato)diboron (13.6 g , 54.1 mmol) in 1,4-dioxane (100 mL) was added KOAc (10.1 g, 104 mmol). The reaction mixture was degassed with nitrogen for 10 min. $PdCl_2(dppf)\cdot DCM$ (3.30 g, 4.15 mmol) was added and the reaction mixture was allowed to stir at 90 °C for 3 h. The reaction mixture was diluted with EtOAc (300 mL) and filtered through a pad of Celite. The filtrate was concentrated under reduced pressure to obtain the crude material which was purified by column chromatography (neutral alumina, gradient: 0-10% EtOAc in hexanes) to obtain 3-chloro-2-isobutoxy-5-(4,4,5,5-tetramethyl-1,3,2-dioxaborolan-2-yl)pyridine **47** (6.0 g, 47% yield) as a colorless oil. MS (ESI, positive ion) m/z: no ionization. ^{1}H NMR (400 MHz, $CDCl_3$) δ 8.36 (d, *J* = 1.6 Hz, 1H), 7.96 (d, *J* = 1.6 Hz, 1H), 4.17 (d, *J* = 6.7 Hz, 2H), 2.14 (dt, *J* = 13.4, 6.7 Hz, 1H), 1.35 (s, 12H), 1.03 (d, *J* = 6.7 Hz, 6H). STEP 3: To a solution of **47** (5.00 g, 16.0 mmol) in acetone (100 mL) was added a solution of oxone (9.80 g, 16.0 mmol) in H_2O (100 mL) at 0 °C and the mixture was allowed to stir for 30

min. The reaction mixture was diluted with EtOAc (500 mL) and washed with water (500 mL). The organic layer was dried over sodium sulfate and concentrated under reduced pressure to obtain the crude material which was purified by column chromatography (silica gel 100-200 mesh, gradient: 0-15% EtOAc in hexanes) to obtain 5-chloro-6-isobutoxypyridin-3-ol **48** (3.5 g, 65% yield) as an off-white solid. MS (ESI, positive ion) m/z: 202.0 $[M+1]^+$. ^{1}H NMR (400 MHz, DMSO-d_6) δ 9.68 (s, 1H), 7.64 (d, J = 2.6 Hz, 1H), 7.33 (d, J = 2.7 Hz, 1H), 3.99 (d, J = 6.7 Hz, 2H), 2.00 (dp, J = 13.3, 6.7 Hz, 1H), 0.95 (d, J = 6.7 Hz, 6H). STEP 4: Using General Procedure A, coupling of **45** and **48** afforded the title compound (175 mg**,** 37% yield) as an off-white solid. MS (ESI, positive ion) m/z: 450.0 $[M+1]^+$. ^{1}H NMR (400 MHz, DMSO-d_6) δ 8.57 (s, 1 H), 8.39 (d, J = 8.70 Hz, 1 H), 8.14 - 8.25 (m, 2 H), 8.10 (d, J = 2.54 Hz, 1 H), 7.98 (d, J = 5.77 Hz, 1 H), 7.67 (d, J = 5.67 Hz, 1 H), 4.16 (d, J = 6.65 Hz, 2 H), 3.16 (s, 3 H), 2.10 (dt, J = 13.23, 6.64 Hz, 1 H), 1.01 (d, J = 6.75 Hz, 6 H). ^{13}C NMR (126 MHz, DMSO-d6) δ 167.4, 159.6, 155.8, 144.1, 139.7, 138.3, 137.7, 137.5, 134.0, 127.1, 126.9, 123.4, 119.5, 117.7, 116.5, 72.7, 40.8, 27.4, 18.9. HRMS m/z: Calcd for $C_{20}H_{20}ClN_3O_5S$: $[M+1]^+$ = 450.089. Found $[M+1]^+$ = 450.0884.

3',4'-Dichloro-*N*-(methylsulfonyl)-4-biphenylcarboxamide (7a). Using General Procedure B, **7a** was prepared from 3',4'-dichloro-[1,1'-biphenyl]-4-carboxylic acid. (100 mg, 58% yield) MS (ESI, positive ion) m/z: 344.7 $[M+2]^+$. ^{1}H NMR (500 MHz, DMSO-d_6) δ 8.20 (br s, 1H), 7.94-8.09 (m, 2H), 7.65-7.78 (m, 3H), 3.14 (s, 3H). ^{13}C NMR (126 MHz, DMSO-d6) δ 166.0, 141.8, 139.2, 131.9, 131.3, 131.2, 131.1, 129.2, 128.8, 127.2, 126.9, 41.3. HRMS m/z: Calcd for $C_{14}H_{11}C_{l2}NO_3S$: $[M+1]^+$ = 343.9915. Found $[M+1]^+$ = 343.9916.

3',4'-Dichloro-2,5-difluoro-*N*-(methylsulfonyl)-4-biphenylcarboxamide (8). Reaction of 4-bromo-2,5-difluoro-*N*-(methylsulfonyl)benzamide **52b** (prepared according to STEP 1 of the

synthesis of **9**) and 3,4-dichlorophenylboronic acid, under similar Suzuki conditions as for STEP 2 of **9** afforded the title compound (78.3 mg, 54% yield) as a white solid. MS (ESI, negative ion) m/z: 379.8 $[M-1]^-$. ^{1}H NMR (500 MHz, DMSO-d_6) δ 7.89 (s, 1H), 7.75 (br d, J = 8.42 Hz, 1H), 7.61 (br d, J = 8.36 Hz, 1H), 7.52 (br dd, J = 5.93, 11.08 Hz, 1H), 7.43 (br dd, J = 6.16, 10.45 Hz, 1H), 2.87 (s, 3H). ^{13}C NMR (126 MHz, DMSO-d6) δ 166.8, 157.1, 155.1, 155.0, 153.1, 134.3, 131.4, 131.2, 130.8, 130.6, 129.1, 117.9, 117.7, 40.3. HRMS m/z: Calcd for $C_{14}H_9C_{l2}F_2NO_3S$: $[M-1]^-$ = 379.9727. Found $[M-1]^-$ = 379.9727.

4-(5-Chloro-6-isobutoxypyridin-3-yl)-2,5-difluoro-*N*-(methylsulfonyl)benzamide (9). STEP 1: A round bottom flask was charged with 4-bromo-2,5-difluorobenzoic acid **51b** (10.00 g, 42.2 mmol), methanesulfonamide (4.82 g, 50.6 mmol), DMAP (11.34 g, 93 mmol), and EDC·HCl (16.18 g, 84 mmol) and CH_2Cl_2 (150 mL) was added. After stirring for 2 d at RT, the mixture was concentrated under reduced pressure to afford the crude material which was dissolved in 500 mL CH_2Cl_2 and 10 mL MeOH and filtered over 25 micron filter paper. The crude solution was injected onto a 1500 g silica gel cartridge (40-63 micron) and eluted at 300 mL/min with a gradient over ten column volumes (15 L total volume) from 2/98/0.1 MeOH/CH_2Cl_2/formic acid to 20/80/1 MeOH/CH_2Cl_2/formic acid to afford 4-bromo-2,5-difluoro-N-(methylsulfonyl)benzamide **52c** (9.78 g, 73.8% yield). MS (ESI, negative ion) m/z: 311 $(M-1)^-$. STEP 2: A resealable 2 dram screw cap reaction vial was charged with **52c** (100 mg, 0.318 mmol), K_2CO_3 (132 mg, 0.955 mmol), $Pd(PPh_3)_4$ (36.8 mg, 0.032 mmol), and **47** (146 mg, 0.637 mmol). The vial was flushed with Ar (g), then 1,4-dioxane (2 mL) and H_2O (0.67 mL) were added. The vial was purged with Ar (g), sealed and heated with shaking at 60 °C overnight. The crude reaction mixture was filtered through a Celite plug and purified by reversed phase preparative LC/MS: Column: Xbridge (19 x 100 mm, C18, 10 μm); flow rate: 40

mL/min; 10 min gradient 5 – 95% CH_3CN / 0.1% NH_4OH in H_2O to afford the title compound (33.6 mg, 25% yield) as a white solid. MS (ESI, positive ion) m/z: 419.0 $[M+1]^+$. ^1H NMR (500 MHz, DMSO-d_6) δ 8.37 (s, 1 H), 8.18 (s, 1H), 7.48 - 7.70 (m, 2 H), 4.19 (d, J = 6.64 Hz, 2H), 3.09 (s, 3 H), 1.97 - 2.19 (m, 1H), 1.00 (d, J = 6.76 Hz, 6H). ^{13}C NMR (126 MHz, DMSO-d6) δ 162.4, 158.6, 156.6, 155.4, 154.6, 153.4, 145.1, 138.8, 123.3, 118.1, 117.8, 117.1, 72.8, 41.2, 27.4, 18.9. HRMS m/z: Calcd for $C_{17}H_{17}ClF_2N_2O_4S$: $[M+1]^+$ = 419.0644. Found $[M+1]^+$ = 419.065.

4-(5-Chloro-6-isobutoxypyridin-3-yl)-2-fluoro-*N*-(methylsulfonyl)benzamide (10). STEP 1: A round bottom flask was charged with 2-fluoro-4-(4,4,5,5-tetramethyl-1,3,2-dioxaborolan-2-yl)benzoic acid **55** (1.0 g, 3.76 mmol), methanesulfonamide (0.715 g, 7.52 mmol), DMAP (1.377 g, 11.28 mmol), and EDC·HCl (1.441 g, 7.52 mmol). CH_2Cl_2 (15 mL) and DMF (5 mL) were added. After stirring for 2 d at RT, the crude reaction mixture was concentrated then purified by reversed phase preparative LC/MS: Column: Xbridge (19 x 100 mm, C18, 10 μm); flow rate: 40 mL/min; 10 min gradient 5 – 95% CH_3CN / 0.1% NH_4OH in H_2O to afford 2-fluoro-*N*-(methylsulfonyl)-4-(4,4,5,5-tetramethyl-1,3,2-dioxaborolan-2-yl)benzamide **56** (0.444 g, 34% yield). MS (ESI, negative ion) m/z: 342 $[M-1]^-$. STEP 2: **56** (0.100 g, 0.291 mmol), 5-bromo-3-chloro-2-isobutoxypyridine (0.093 g, 0.350 mmol), K_2CO_3 (0.121 g, 0.874 mmol), and $Pd(PPh_3)_4$ (0.034 g, 0.029 mmol) were combined in a 2 dram resealable screw cap reaction vial. 1,4-dioxane (3 mL) and H_2O (1.00 mL) were added. The mixture was purged with Ar (g), the vial was capped and heated at 60 °C with shaking overnight. After concentrating, the crude product was purified by reversed phase preparative LC/MS: Column: Xbridge (19 x 100 mm, C18, 10 μm); flow rate: 40 mL/min; 10 min gradient 5 – 95% CH_3CN / 0.1% NH_4OH in H_2O to afford the title compound (51.2 mg, 44% yield) as a white solid. MS (ESI, positive ion) m/z: 401.1

[M+1]$^+$. ^{1}H NMR (400 MHz, DMSO-d_6) δ 8.53 (d, J = 2.25 Hz, 1H), 8.34 (d, J = 2.25 Hz, 1H), 7.75 (t, J = 8.02 Hz, 1H), 7.54 - 7.64 (m, 2H), 4.19 (d, J = 6.65 Hz, 2H), 3.00 (s, 3H), 2.04 - 2.14 (m, 1H), 1.01 (d, J = 6.65 Hz, 6H). ^{13}C NMR (126 MHz, DMSO-d6) δ 165.1, 161.2, 159.2, 158.5, 143.3, 140.3, 137.0, 131.2, 128.1, 121.9, 117.5, 114.1, 72.7, 41.0, 27.4, 18.9. HRMS m/z: Calcd for $C_{17}H_{18}ClFN_2O_4S$: [M+1]$^+$ = 401.0738. Found [M+1]$^+$ = 401.0743.

4-(5-Chloro-6-(2-methylpropoxy)-3-pyridinyl)-3-fluoro-*N*-(methylsulfonyl)benzamide (11). Reaction of 4-bromo-3-fluorobenzoic acid **51d** and methanesulfonamide, under similar DMAP/EDC·HCl coupling conditions as for STEP 1 of **9** afforded 4-bromo-3-fluoro-*N*-(methylsulfonyl)benzamide **52d**, which was coupled to **47**, under similar Suzuki conditions as for STEP 2 of **9** to afford the title compound (108 mg, 66.5% yield) as a white solid. MS (ESI, positive ion) m/z: 401.1 [M+1]$^+$. ^{1}H NMR (400 MHz, DMSO-d_6) δ 8.34 (t, J = 1.81 Hz, 1H), 8.10 - 8.18 (m, 1H), 7.84 (dd, J = 7.97, 1.52 Hz, 1H), 7.75 (dd, J = 12.03, 1.37 Hz, 1H), 7.60 (t, J = 7.97 Hz, 1H), 4.19 (d, J = 6.65 Hz, 2H), 2.93 (s, 3H), 2.09 (dt, J = 13.40, 6.70 Hz, 1H), 1.00 (d, J = 6.75 Hz, 6H). HRMS m/z: Calcd for $C_{17}H_{18}ClFN_2O_4S$: [M+1]$^+$ = 401.0738. Found [M+1]$^+$ = 401.073.

4-(5-Chloro-6-(2-methylpropoxy)-3-pyridinyl)-*N*-(methylsulfonyl)benzamide (12). Reaction of 4-bromobenzoic acid **51e** and methanesulfonamide, under similar DMAP/EDC·HCl coupling conditions as for STEP 1 of **9** afforded 4-bromo-*N*-(methylsulfonyl)benzamide **51e**, which was coupled to **47**, under similar Suzuki conditions as for STEP 2 of **9** to afford the title compound (107 mg, 64.8% yield) as a white solid. MS (ESI, positive ion) m/z: 383 [M+1]$^+$. ^{1}H NMR (400 MHz, DMSO-d_6) δ 12.20 (br s, 1H), 8.51 (d, J = 2.25 Hz, 1H), 8.31 (d, J = 2.25 Hz, 1H), 8.00-8.04 (m, 2H), 7.75-7.81 (m, J = 8.31 Hz, 2H), 4.19 (d, J = 6.65 Hz, 2H), 3.05-3.14 (m, 3H), 2.10 (quind, J = 6.58, 13.31 Hz, 1H), 1.01 (d, J = 6.75 Hz, 6H). ^{13}C NMR (126 MHz, DMSO-d6) δ

167.9, 158.1, 143.0, 138.2, 136.9, 135.2, 129.6, 129.0, 125.9, 117.4, 72.6, 40.8, 27.4, 18.9. HRMS m/z: Calcd for $C_{17}H_{19}ClN_2O_4S$: $[M+1]^+$ = 383.0832. Found $[M+1]^+$ = 383.0824.

4-(5-Chloro-6-(2-methylpropoxy)-3-pyridinyl)-2-methyl-*N*-(methylsulfonyl)benzamide (13). Reaction of 4-bromo-2-methylbenzoic acid **51f** and methanesulfonamide, under similar DMAP/EDC·HCl coupling conditions as for STEP 1 of **9** afforded 4-bromo-2-methyl-*N*-(methylsulfonyl)benzamide **52f**, which was coupled to **47**, under similar Suzuki conditions as for STEP 2 of **9** to afford the title compound (163 mg, 37.7% yield) as a white solid. MS (ESI, positive ion) m/z: 397 $[M+1]^+$. ^{1}H NMR (400 MHz, DMSO-d_6) δ 12.15 (br s, 1H), 8.51 (d, J = 2.25 Hz, 1H), 8.31 (d, J = 2.25 Hz, 1H), 7.71 (s, 1H), 7.66 (d, J = 7.75 Hz, 1H), 7.58 (d, J = 7.63 Hz, 1H), 4.19 (d, J = 6.65 Hz, 2H), 3.40 (s, 3H), 2.47 (s, 3H), 2.04 - 2.15 (m, 1H), 1.01 (d, J = 6.65 Hz, 6H). ^{13}C NMR (126 MHz, DMSO-d6) δ 168.2, 158.2, 143.1, 138.0, 137.5, 136.9, 132.5, 129.2, 128.9, 128.8, 123.5, 117.4, 72.7, 41.2, 27.4, 19.6, 18.9. HRMS m/z: Calcd for $C_{18}H_{21}ClN_2O_4S$: $[M+1]^+$ = 397.0989. Found $[M+1]^+$ = 397.0983.

2-Chloro-4-(5-chloro-6-(2-methylpropoxy)-3-pyridinyl)-*N*-(methylsulfonyl)benzamide (14). Reaction of 4-bromo-2-chlorobenzoic **51g** acid and methanesulfonamide, under similar DMAP/EDC·HCl coupling conditions as for STEP 1 of **9** afforded 4-bromo-2-chloro-*N*-(methylsulfonyl)benzamide **52g**, which was coupled to **47**, under similar Suzuki conditions as for STEP 2 of **9** to afford the title compound (80 mg, 60% yield) as a light yellow solid. MS (ESI, negative ion) m/z: 416.0 $[M]^-$. ^{1}H NMR (500 MHz, DMSO-d_6) δ 8.47 (d, J = 2.03 Hz, 1H) 8.28 (d, J = 1.98 Hz, 1H) 7.72 (s, 1H) 7.62 (d, J = 7.96 Hz, 1H) 7.54 (d, J = 7.96 Hz, 1H) 4.17 (d, J = 6.57 Hz, 2H) 2.90 (s, 3H) 2.00 - 2.14 (m, 1H) 0.92 - 1.04 (m, 6H). ^{13}C NMR (126 MHz, DMSO-d6) δ 170.0, 158.1, 143.0, 139.3, 136.9, 136.5, 130.9, 129.8, 128.7, 127.2, 124.4, 117.4, 72.6,

40.3, 27.4, 18.9. HRMS m/z: Calcd for $C_{17}H_{18}C_{l2}N_2O_4S$: $[M+1]^+$ = 417.0443. Found $[M+1]^+$ = 417.044.

4-(5-Chloro-6-(2-methylpropoxy)-3-pyridinyl)-3,5-difluoro-*N*-(methylsulfonyl)benzamide (15). Reaction of 4-bromo-3,5-difluorobenzoic acid **51h** and methanesulfonamide, under similar DMAP/EDC·HCl coupling conditions as for STEP 1 of **9** afforded 4-bromo-3,5-difluoro-*N*-(methylsulfonyl)benzamide **52h**, which was coupled to **47**, under similar Suzuki conditions as for STEP 2 of **9** to afford the title compound (75 mg, 55.8% yield) as a white solid. MS (ESI, positive ion) m/z: 419 $[M+1]^+$. ^{1}H NMR (500 MHz, DMSO-d_6) δ 8.24 (s, 1H), 8.08 (s, 1H), 7.62 (d, J = 8.60 Hz, 2H), 4.19 (d, J = 6.57 Hz, 2H), 2.88 (s, 3H), 2.03 - 2.15 (m, 1 H), 1.00 (d, J = 6.68 Hz, 6H). ^{13}C NMR (126 MHz, DMSO-d6) δ 166.8, 159.8, 158.3, 157.8, 145.9, 142.7, 139.9, 118.9, 116.8, 111.2, 72.7, 40.2, 27.4, 18.9. HRMS m/z: Calcd for $C_{17}H_{17}ClF_2N_2O_4S$: $[M+1]^+$ = 419.0644. Found $[M+1]^+$ = 419.0642.

5'-Chloro-3-fluoro-6'-(2-methylpropoxy)-*N*-(methylsulfonyl)-2,3'-bipyridine-5-carboxamide (16). Reaction of 6-bromo-5-fluoronicotinic acid **51i** and methanesulfonamide, under similar DMAP/EDC·HCl coupling conditions as for STEP 1 of **9** afforded 6-bromo-5-fluoro-*N*-(methylsulfonyl)nicotinamide **52i**, which was coupled to **47**, under similar Suzuki conditions as for STEP 2 of **9** to afford the title compound (106 mg, 65.3% yield) as a white solid. MS (ESI, negative ion) m/z: 400.2 $[M-1]^-$. ^{1}H NMR (400 MHz, DMSO-d_6) δ 8.97 (t, J = 1.76 Hz, 1H), 8.69 (s, 1H), 8.42 (dd, J = 0.73, 2.10 Hz, 1H), 8.06 (dd, J = 1.57, 12.13 Hz, 1H), 4.23 (d, J = 6.65 Hz, 2H), 2.91 (s, 3H), 2.11 (td, J = 6.66, 13.38 Hz, 1H), 1.02 (d, J = 6.65 Hz, 7H). ^{13}C NMR (126 MHz, DMSO-d6) δ 166.7, 158.8, 157.6, 145.7, 145.1, 141.8, 138.1, 135.9, 125.4, 123.6, 117.2, 72.9, 40.4, 27.4, 18.9. HRMS m/z: Calcd for $C_{16}H_{17}ClFN_3O_4S$: $[M+1]^+$ = 402.0691. Found $[M+1]^+$ = 402.0685.

3-Chloro-4-(5-chloro-6-(2-methylpropoxy)-3-pyridinyl)-*N*-(methylsulfonyl)benzamide (17). Reaction of 4-bromo-3-chlorobenzoic acid **51j** and methanesulfonamide, under similar DMAP/EDC·HCl coupling conditions as for STEP 1 of **9** afforded 4-bromo-3-chloro-*N*-(methylsulfonyl)benzamide **52j**, which was coupled to **47** under similar Suzuki conditions as for STEP 2 of **9** to afford the title compound (72 mg, 53.8% yield) as a white solid. MS (ESI, positive ion) m/z: 418.2 $[M+2]^+$. ^{1}H NMR (400 MHz, DMSO-d_6) δ 8.24 (d, J = 2.15 Hz, 1 H), 8.16 (d, J = 1.76 Hz, 1 H), 8.10 (d, J = 2.15 Hz, 1 H), 7.97 (dd, J = 8.07, 1.81 Hz, 1 H), 7.66 (d, J = 8.02 Hz, 1 H), 4.19 (d, J = 6.65 Hz, 2 H), 2.04 - 2.16 (m, 1 H), 1.01 (d, J = 6.65 Hz, 6 H). ^{13}C NMR (126 MHz, DMSO-d6) δ 167.7, 157.9, 144.9, 140.4, 139.3, 136.3, 131.0, 130.9, 129.4, 128.6, 127.2, 116.4, 72.7, 40.3, 27.4, 18.9. HRMS m/z: Calcd for $C_{17}H_{18}C_{l2}N_2O_4S$: $[M+1]^+$ = 417.0443. Found $[M+1]^+$ = 417.0447.

4-(5-Chloro-6-(2-methylpropoxy)-3-pyridinyl)-*N*-(methylsulfonyl)-3-(trifluoromethyl)benzamide (18). Reaction of 4-bromo-3-(trifluoromethyl)benzoic acid **51k** and methanesulfonamide, under similar DMAP/EDC·HCl coupling conditions as for STEP 1 of **9** afforded 4-bromo-*N*-(methylsulfonyl)-3-(trifluoromethyl)benzamide **52k**, which was coupled to **47**, under similar Suzuki conditions as for STEP 2 of **9** to afford the title compound (130 mg, 66.8%) as a white solid. MS (ESI, positive ion) m/z: 451 $[M+1]^+$. ^{1}H NMR (500 MHz, DMSO-d_6) δ 8.36 (s, 1H), 8.22 (br d, J = 7.80 Hz, 1H), 8.07 (d, J = 1.66 Hz, 1H), 7.90 - 7.97 (m, 1H), 7.39 - 7.50 (m, 1H), 4.18 (d, J = 6.57 Hz, 2H), 2.88 (s, 3H), 2.09 (td, J = 6.66, 13.34 Hz, 1H), 1.01 (d, J = 6.68 Hz, 6H). ^{13}C NMR (126 MHz, DMSO-d6) δ 167.9, 158.1, 144.2, 139.9, 138.9, 136.6, 132.3, 131.7, 129.1, 126.6, 125.8, 125.2, 116.3, 72.7, 40.2, 27.4, 18.9. HRMS m/z: Calcd for $C_{18}H_{18}ClF_3N_2O_4S$: $[M+1]^+$ = 451.0706. Found $[M+1]^+$ = 451.0697.

4-(5-Chloro-6-isobutoxypyridin-3-yl)-3-(2,5-dihydrofuran-3-yl)-*N*-(methylsulfonyl)benzamide (19). STEP 1: A suspension of EDC·HCl (0.586 g, 3.06 mmol), DMAP (0.561 g, 4.59 mmol), methanesulfonamide (0.128 mL, 1.835 mmol) and 3-bromo-4-iodobenzoic acid **57** (0.5 g, 1.529 mmol) in CH_2Cl_2 (5 mL) was stirred at RT for 16 h. The reaction mixture was concentrated and purified by reversed phase preparative LC/MS: Column: Xbridge (19 x 100 mm, C18, 10 μm); flow rate: 40 mL/min; 10 min gradient 5 – 95% CH_3CN / 0.1% TFA in H_2O to obtain 3-bromo-4-iodo-*N*-(methylsulfonyl)benzamide **58** (0.268 g, 43.4 % yield) as a white solid. MS (ESI, positive ion) m/z: 405.0 $[M+1]^+$. STEP 2: To a vial charged with 3-chloro-2-isobutoxypyridine-5-boronic acid (0.710 g, 3.09 mmol), **58** (2.5 g, 6.19 mmol), and Na_2CO_3 (1.968 g, 18.56 mmol) was added 1,4-dioxane (24.75 mL), *t*-BuOH (24.75 mL) and H_2O (12.38 mL). $PdCl_2(dppf)\cdot DCM$ (0.505 g, 0.619 mmol), and $Pd_2(dba)_3$ (0.505 g) were added. The mixture was purged with Ar (g) and heated to 50 °C for 30 min. The reaction mixture was then diluted with CH_2Cl_2 (200 mL) and H_2O (100 mL) and 2N HCl (100 mL) was added. The organic layer was separated and concentrated then purified by MPLC (Biotage Isolera One; PuriFlash HP; EtOAc in heptanes) to obtain 3-bromo-4-(5-chloro-6-isobutoxypyridin-3-yl)-N-(methylsulfonyl)benzamide **59** (1.41 g, 3.05 mmol, 49.3 % yield) as an off-white solid. MS (ESI, positive ion) m/z: 461.0 $(M+1)^+$. A resealable screw cap vial charged with a suspension of Na_2CO_3 (0.027 mL, 0.65 mmol), $PdCl_2(dppf)\cdot DCM$ (0.02 g, 0.02 mmol), $Pd_2(dba)_3$ (0.02 g, 0.02 mmol), 2-(2,5-dihydrofuran-3-yl)-4,4,5,5-tetramethyl-1,3,2-dioxaborolane (0.04 g, 0.25 mmol) and **59** (0.1 g, 0.22 mmol) in 1,4-dioxane (1 mL), *t*-BuOH (0.5 mL), and water (0.5 mL) was purged with nitrogen and was heated with shaking at 95 °C for 1.5 h. The organic layer was decanted and filtered through a Celite plug, and concentrated under reduced pressure. The crude material was purified by reversed phase preparative LC/MS: Column: Xbridge (19 x 100 mm,

C18, 10 μm); flow rate: 40 mL/min; 10 min gradient 5 – 95% CH_3CN / 0.1% NH_4OH in H_2O to afford the title compound to obtain title compound (8 mg, 12% yield) as light yellow solid. MS (ESI, positive ion) m/z: 451.0 $(M+H)^+$. ^1H NMR (500 MHz, DMSO-d_6) δ ppm 8.08 (s, 1 H) 7.89 - 7.98 (m, 2 H) 7.60 (d, *J* = 16.40 Hz, 1 H) 7.33 - 7.49 (m, 1 H) 5.79 (br. s., 1 H) 4.58 (br. s., 1 H) 4.47 (br. s., 1 H) 4.12 - 4.24 (m, 2 H) 2.91 - 3.00 (m, 3 H) 2.54 (s, 1 H) 2.08 (dt, *J*=13.08, 6.63 Hz, 1 H) 0.94 - 1.10 (m, 6 H); HRMS m/z: Calcd for $C_{21}H_{23}ClN_2O_5S$ $[M+1]^+$ = 451.1094. Found $[M+1]^+$ = 451.1090.

4-(5-Chloro-6-(2-methylpropoxy)-3-pyridinyl)-*N*-(methylsulfonyl)-3-(trifluoromethoxy)benzamide (20). Reaction of 4-bromo-3-(trifluoromethoxy)benzoic acid **51l** and methanesulfonamide, under similar DMAP/EDC·HCl coupling conditions as for STEP 1 of **9** afforded 4-bromo-*N*-(methylsulfonyl)-3-(trifluoromethoxy)benzamide **52l**, which was coupled to **47**, under similar Suzuki conditions as for STEP 2 of **9** to afford the title compound (71 mg, 55.1% yield) as a white solid. MS (ESI, negative ion) m/z: 465 $[M-1]^-$. ^1H NMR (500 MHz, DMSO-d_6) δ 8.25 (d, *J* = 1.98 Hz, 1H), 8.07 (d, *J* = 2.03 Hz, 1H), 8.01 (br d, *J* = 7.91 Hz, 1H), 7.95 (br s, 1H), 7.58 (br d, *J* = 7.96 Hz, 1H), 4.18 (d, *J* = 6.57 Hz, 2H), 3.17 (d, *J* = 5.02 Hz, 1H), 2.88 (s, 3H), 2.04-2.13 (m, 1H), 1.00 (d, *J* = 6.73 Hz, 6H). ^{13}C NMR (126 MHz, DMSO-d6) δ 167.9, 158.0, 144.9, 144.8, 141.6, 138.9, 130.8, 127.4, 126.2, 121.0, 120.5, 119.0, 116.7, 72.7, 40.2, 27.4, 18.9. HRMS m/z: Calcd for $C_{18}H_{18}ClF_3N_2O_5S$ $[M+1]^+$ = 467.0655. Found $[M+1]^+$ = 467.0656.

4-(5-Chloro-6-(2-methylpropoxy)-3-pyridinyl)-3-methoxy-*N*-(methylsulfonyl)benzamide (21). Reaction of 4-bromo-3-methoxybenzoic acid **51m** and methanesulfonamide, under similar DMAP/EDC·HCl coupling conditions as for STEP 1 of **9** afforded 4-bromo-3-methoxy-*N*-(methylsulfonyl)benzamide **52m**, which was coupled to **47**, under similar Suzuki conditions as

for STEP 2 of **9** to afford the title compound (48.7 mg, 37% yield) as a white solid. MS (ESI, positive ion) m/z: 413 $[M+1]^+$. ^{1}H NMR (500 MHz, DMSO-d_6) δ 8.24 (d, J = 2.03 Hz, 1 H), 8.03 (d, J = 1.92 Hz, 1 H), 7.67 (s, 1 H), 7.62 (d, J = 7.91 Hz, 1 H), 7.36 (d, J = 7.91 Hz, 1 H), 4.17 (d, J = 6.52 Hz, 2 H), 3.83 (s, 3 H), 2.97 (s, 3 H), 2.01 - 2.15 (m, 1 H), 1.00 (d, J = 6.62 Hz, 6 H). ^{13}C NMR (126 MHz, DMSO-d6) δ 165.2, 157.6, 157.3, 145.9, 139.1, 134.1, 134.0, 130.0, 127.5, 123.1, 122.5, 110.0, 73.6, 56.0, 41.1, 28.0, 19.1. HRMS m/z: Calcd for $C_{18}H_{21}ClN_2O_5S$ $[M+1]^+$ = 413.0938. Found $[M+H]^+$ = 413.0936.

4-(5-Chloro-6-(2-methylpropoxy)-3-pyridinyl)-3-cyano-*N*-(methylsulfonyl)benzamide (22). Reaction of 4-bromo-3-cyanobenzoic acid **51n** and methanesulfonamide, under similar DMAP/EDC·HCl coupling conditions as for STEP 1 of **9** afforded 4-bromo-3-cyano-*N*-(methylsulfonyl)benzamide **52n**, which was coupled to **47**, under similar Suzuki conditions as for STEP 2 of **9** to afford the title compound (60 mg, 37.2% yield) as a white solid. MS (ESI, positive ion) m/z: 408.2 $[M+1]^+$. ^{1}H NMR (400 MHz, DMSO-d_6) δ 8.37 - 8.40 (m, 2H), 8.24-8.28 (m, 2H), 7.74 (d, J = 8.12 Hz, 1H), 4.22 (d, J = 6.65 Hz, 2H), 3.04 (s, 3H), 2.11 (td, J = 6.66, 13.38 Hz, 1H), 1.02 (d, J = 6.75 Hz, 6H). ^{13}C NMR (126 MHz, DMSO-d6) δ 164.3, 159.3, 147.7, 146.2, 139.4, 135.0, 134.1, 130.2, 129.2, 128.8, 123.2, 114.1, 113.4, 73.6, 41.1, 28.0, 19.1. HRMS m/z: Calcd for $C_{18}H_{18}ClN_3O_4S$ $[M+1]^+$ = 408.0785. Found $[M+1]^+$ = 408.0783.

4-(5-Chloro-6-(2-methylpropoxy)-3-pyridinyl)-*N3,N3*-dimethyl-*N1*-(methylsulfonyl)-1,3-benzenedicarboxamide (23). Reaction of 4-bromo-3-(dimethylcarbamoyl)benzoic acid **51o** and methanesulfonamide, under similar DMAP/EDC·HCl coupling conditions as for STEP 1 of **9** afforded 4-bromo-*N3,N3*-dimethyl-*N1*-(methylsulfonyl)isophthalamide **52o**, which was coupled to **47**, under similar Suzuki conditions as for STEP 2 of **9** to afford the title compound (42 mg, 44% yield) as a white solid. MS (ESI, positive ion) m/z: 454.1 $[M+1]^+$. ^{1}H NMR (500 MHz,

DMSO-d_6) δ 8.12 (d, J = 2.08 Hz, 1H), 8.01 (dd, J = 8.01, 1.55 Hz, 1H), 7.89 (br d, J = 2.08 Hz, 1H), 7.81 (br d, J = 1.39 Hz, 1H), 7.49 (d, J = 8.01 Hz, 1H), 4.16 (d, J = 6.57 Hz, 2H), 2.88 (s, 3H), 2.85 (s, 3H), 2.55 (s, 3H), 2.08 (dt, J = 13.32, 6.67 Hz, 1H), 1 (d, J = 6.73 Hz, 6H). ^{13}C NMR (126 MHz, DMSO-d6) δ 169.5, 168.1, 157.9, 143.9, 138.0, 135.2, 134.8, 131.1, 129.4, 129.1, 128.9, 127.0, 116.7, 72.7, 40.5, 37.8, 34.0, 27.4, 18.9. HRMS m/z: Calcd for $C_{20}H_{24}ClN_3O_5S$ $[M+1]^+$ = 454.1203. Found $[M+1]^+$ = 454.1198.

4-(5-Chloro-6-fluoro-3-pyridinyl)-3-methoxy-*N*-(methylsulfonyl)benzamide (24). STEP 1: To a flask charged with 4-bromo-3-methoxybenzoic acid **51p** (9.971 g, 43.2 mmol) was added DMAP (7.91 g, 64.7 mmol), methanesulfonamide (4.93 g, 51.8 mmol), CH_2Cl_2 (173 mL) and EDC-HCl (12.41 g, 64.7 mmol) respectively. The mixture was stirred overnight at RT, transferred to a separatory funnel and washed with 2N HCl. The CH_2Cl_2 layer was dried with Na_2SO_4, filtered, and concentrated under reduced pressure to afford 4-bromo-3-methoxy-N-(methylsulfonyl)benzamide **52p** (12.88 g, 97% yield) as a white solid. MS (ESI, positive ion) m/z: 330.0 $[M+Na]^+$. STEP 2: To a flask charged with **52p** (10 g, 32.5 mmol), **47** (8.36 g, 32.5 mmol), and $Pd(PPh_3)_4$ (1.875 g, 1.623 mmol) was added 1,4-dioxane (130 mL) and Na_2CO_3 (2M aq.) (81 mL, 162 mmol) and the mixture purged with nitrogen for 5 min then heated to 100 °C for 4 h. The suspension was cooled in an ice water bath and brought to pH < 2 by the addition of 6N HCl. The mixture was stirred at 0 °C for 10 min affording a white precipitate. The mixture was cooled overnight in the 4 °C fridge and the while solid collected by vacuum filtration and dried under a vacuum/nitrogen sweep to afford the title compound (8.11 g, 69.7% yield) as a white solid. MS (ESI, positive ion) m/z: 359.1 $[M+1]^+$. ^{1}H NMR (400 MHz, DMSO-d_6) δ 12.18 (br s, 1H), 8.25 - 8.32 (m, 2H), 7.61 (d, J = 1.56 Hz, 1H), 7.54 - 7.59 (m, 1H), 7.46 - 7.52 (m,

1H), 3.80 (s, 3H). HRMS m/z: Calcd for $C_{14}H_{12}ClFN_2O_4S$ $[M+1]^+$ = 359.0269. Found $[M+1]^+$ = 359.0271.

4-(5-Chloro-6-(3,5-dichlorophenoxy)-3-pyridinyl)-3-methoxy-N-(methylsulfonyl)benzamide (25). Using General Procedure C, reaction of **24** and 3,5-dichlorophenol at 90 ºC afforded the title compound (55.4 mg, 79 % yield). MS (ESI, positive ion) m/z: 501.0 $[M+H]^+$. ^{1}H NMR (500 MHz, DMSO-d_6) δ 8.26 (d, *J* = 1.98 Hz, 1H), 8.23 (d, *J* = 2.03 Hz, 1H), 7.68 (s, 1H), 7.62 (d, *J* = 7.85 Hz, 1H), 7.52 (t, *J* = 1.68 Hz, 1H), 7.32 - 7.47 (m, 3H), 3.83 (s, 4H), 2.92 (s, 3H). ^{13}C NMR (126 MHz, DMSO-d6) δ 168.9, 156.3, 155.5, 154.6, 145.1, 140.5 140.4, 134.5, 131.0, 129.5, 125.7, 125.1, 121.1, 121.0, 117.2, 111.2, 55.6, 40.4. HRMS m/z: Calcd for $C_{20}H_{15}Cl_3N_2O_5S$ $[M+1]^+$ = 500.9846. Found $[M+1]^+$ = 500.9846.

4-(5-Chloro-6-(2,5-difluorophenoxy)-3-pyridinyl)-3-methoxy-*N*-(methylsulfonyl)benzamide (26). Using General Procedure C, reaction of **24** and 2,5-difluorophenol at 90 ºC afforded the title compound (40 mg, 61% yield). MS (ESI, positive ion) m/z: 469.0 $[M+1]^+$. ^{1}H NMR (500 MHz, DMSO-d_6) δ 8.23 (dd, *J* = 1.98, 14.64 Hz, 2H), 7.68 (s, 1H), 7.63 (d, *J* = 7.86 Hz, 1H), 7.45-7.52 (m, 2H), 7.43 (d, *J* = 7.86 Hz, 1H), 7.21 (t, *J* = 8.59 Hz, 1H), 3.85 (s, 3H), 3.08 (s, 3H). ^{13}C NMR (126 MHz, DMSO-d6) δ 167.7, 159.0, 157.0, 156.1, 155.7, 151.7, 149.8, 145.1, 140.5, 130.5, 129.9, 126.8, 121.1, 117.5, 116.2, 113.3, 112.1, 111.3, 55.8, 40.7. HRMS m/z: Calcd for $C_{20}H_{15}ClF_2N_2O_5S$ $[M+Na]^+$ = 491.0255. Found $[M+1]^+$ = 491.0250.

4-(5-Chloro-6-((5-chloro-2-methoxypyridin-3-yl)oxy)pyridin-3-yl)-3-methoxy-*N*-(methylsulfonyl)benzamide (27). Using General Procedure C, reaction of **24** and 5-chloro-2-methoxypyridin-3-ol at 90 ºC afforded the title compound (55 mg, 79% yield). MS (ESI, positive ion) m/z: 498.4 $[M]^+$. ^{1}H NMR (500 MHz, DMSO-d_6) δ 8.21 (d, *J* = 1.98 Hz, 1H), 8.18

(dd, *J* = 2.12, 5.46 Hz, 2H), 7.99 (d, *J* = 2.26 Hz, 1H), 7.67 (s, 1H), 7.62 (dd, *J* = 1.10, 7.89 Hz, 1H), 7.40 (d, *J* = 7.86 Hz, 1H), 3.84 (s, 6H), 3.03 (s, 3H). ^{13}C NMR (126 MHz, DMSO-d6) δ 168.1, 156.3, 155.7, 155.4, 145.0, 141.3, 140.4, 138.4, 136.7, 131.9, 130.3, 129.8, 126.6, 122.8, 121.1, 116.1, 111.2, 55.7, 54.0, 40.6. HRMS m/z: Calcd for $C_{20}H_{17}Cl_2N_3O_6S$ $[M+1]^+$ = 498.0293. Found $[M+H]^+$ = 498.0298.

4-(5-Chloro-6-((4-chlorobenzyl)oxy)-3-pyridinyl)-3-methoxy-*N*-(methylsulfonyl)benzamide (28). Using General Procedure C, reaction of **24** and (4-chlorophenyl)methanol at 120 ºC afforded the title compound (39 mg, 58% yield) as an off-white solid. MS (ESI, negative ion) m/z: 479.0 $[M-1]^-$. ^{1}H NMR (500 MHz, DMSO-d_6) δ 8.27 (d, *J* = 1.98 Hz, 1H), 8.07 (d, *J* = 2.04 Hz, 1H), 7.67 (s, 1H), 7.62 (d, *J* = 7.75 Hz, 1H), 7.44 - 7.55 (m, 4H), 7.34 (d, *J* = 7.80 Hz, 1H), 5.48 (s, 2 H), 3.82 (s, 3H), 2.88 (s, 3H). ^{13}C NMR (126 MHz, DMSO-d6) δ 169.3, 156.7, 155.5, 144.7, 141.0, 139.5, 135.9, 132.5, 129.6, 129.3, 128.7, 128.5, 125.9, 121.0, 116.3, 111.1, 67.0, 55.5, 40.3. HRMS m/z: Calcd for $C_{21}H_{18}Cl_2N_2O_5S$ $[M+1]^+$ = 481.0392. Found $[M+1]^+$ = 481.0377.

4-(5-Chloro-6-((1-methylcyclopropyl)methoxy)-3-pyridinyl)-3-methoxy-N-(methylsulfonyl)benzamide (29). Using General Procedure C, reaction of **24** and (1-methylcyclopropyl)methanol at 120 ºC afforded the title compound (44 mg, 37% yield) as a white solid. MS (ESI, positive ion) m/z: 425.2 $[M+1]^+$. ^{1}H NMR (500 MHz, DMSO-*d*$_6$) δ 8.22 (d, *J* = 7.25 Hz, 1H), 8.02 (d, *J* = 9.15 Hz, 1H), 7.66 (s, 1H), 7.61 (d, *J* = 7.85 Hz, 1H), 7.34 (d, *J* = 7.85 Hz, 1H), 4.19 (s, 2H), 3.82 (s, 3H), 2.92 (s, 3H), 1.20 (s, 3H), 0.53 - 0.60 (m, 2H), 0.35 - 0.45 (m, 2H). ^{13}C NMR (126 MHz, DMSO-d6) δ 169.1, 157.5, 155.5, 144.7, 140.3, 139.2, 129.3, 128.0, 126.3, 121.0, 116.2, 111.2, 74.0, 55.5, 40.3, 20.8, 15.4, 11.0. HRMS m/z: Calcd for $C_{19}H_{21}ClN_2O_5S$ $[M+1]^+$ = 425.0938. Found $[M+1]^+$ = 425.0929.

4-(5-Chloro-6-(cyclobutyloxy)-3-pyridinyl)-3-methoxy-*N*-(methylsulfonyl)benzamide (30). Using General Procedure C, reaction of **24** and cyclobutanol at 120 ºC afforded the title compound (41.4 mg, 46% yield) as a white solid. MS (ESI, positive ion) m/z: 411.0 $[M+1]^+$. ^{1}H NMR (500 MHz, DMSO-*d*6) δ 8.28 (d, *J* = 1.95 Hz, 1H), 8.07 (d, *J* = 1.95 Hz, 1H), 7.72 (s, 1H), 7.67 (d, *J* = 7.85 Hz, 1H), 7.40 (d, *J* = 7.62 Hz, 1H), 5.30 (quin, *J* = 7.38 Hz, 1H), 3.88 (s, 3H), 2.98 (s, 3H), 2.52 - 2.58 (m, 2H), 2.13 - 2.24 (m, 2H), 1.88 (q, *J* = 9.95 Hz, 1H), 1.68 - 1.78 (m, 1H). ^{13}C NMR (126 MHz, DMSO-d6) δ 168.8, 156.6, 155.5, 144.9, 139.5, 139.2, 129.4, 128.0, 126.5, 121.0, 116.1, 111.2, 70.4, 55.6, 40.4, 30.3, 13.0. HRMS m/z: Calcd for $C_{18}H_{19}ClN_2O_5S$ $[M+1]^+$ = 411.0781. Found $[M+1]^+$ = 411.0773.

4-(5-Chloro-6-((3-methylphenyl)sulfanyl)-3-pyridinyl)-3-methoxy-*N*-(methylsulfonyl)benzamide (31). Using General Procedure D, reaction of 3-methylbenzenethiol and **24** afforded the title compound (0.05 g, 26% yield) as a white solid. MS (ESI, positive ion) m/z: 463.0 $[M+1]^+$. ^{1}H NMR (500 MHz, DMSO-d_6) δ 8.42 (d, *J* = 1.75 Hz, 1H), 8.04 (d, *J* = 1.75 Hz, 1H), 7.66 (s, 1H), 7.61 (br d, *J* = 7.98 Hz, 1H), 7.36-7.43 (m, 4H), 7.29 (br d, *J* = 3.63 Hz, 1H), 3.82 (s, 3H), 2.99 (s, 3H), 2.35 (s, 3H). ^{13}C NMR (126 MHz, DMSO-d6) δ 168.4, 155.7, 154.5, 147.7, 139.4, 138.8, 136.9, 135.8, 132.6, 131.5, 130.1, 129.7, 129.2, 128.4, 126.8, 126.3, 121.1, 111.2, 55.7, 40.5, 20.8. HRMS m/z: Calcd for $C_{21}H_{19}ClN_2O_4S_2$ $[M+1]^+$ = 463.0553. Found $[M+1]^+$ = 463.0557.

4-(5-Chloro-6-((2S)-2-(1-methylethyl)-1-pyrrolidinyl)-3-pyridinyl)-3-methoxy-*N*-(methylsulfonyl)benzamide (32). Using General Procedure E, reaction of 2-isopropylpyrrolidine and **24** afforded racemic 4-(5-chloro-6-(2-(1-methylethyl)-1-pyrrolidinyl)-3-pyridinyl)-3-methoxy-*N*-(methylsulfonyl)benzamide (43 mg, 68% yield). Chiral separation conditions: Chiralpak IC (4.6 x 100 mm) column, conditions: 25% 1:1 acetonitrile:MeOH (No

DEA), 75% CO_2, 50 ml/min, 100 bar pressure. The first eluting Peak 1 was concentrated to afford the title compound (Absolute stereochemistry arbitrarily assigned as *S*). MS (ESI, positive ion) m/z: 452.2 $[M+H]^+$. ^{1}H NMR (500 MHz, DMSO-d_6) δ 8.28 (d, J = 2.03 Hz, 1H), 7.84 (d, J = 2.03 Hz, 1H), 7.54 - 7.70 (m, 2H), 7.43 (d, J = 7.91 Hz, 1H), 4.38 - 4.50 (m, 1H), 3.86 (s, 3H), 3.71 - 3.79 (m, 1H), 3.38 - 3.46 (m, 1H), 3.18 (s, 3H), 2.07 - 2.19 (m, 1H), 1.91 (d, J = 4.38 Hz, 2H), 1.63 - 1.74 (m, 2H), 0.86 (d, J = 6.89 Hz, 3H), 0.73 (d, J = 6.79 Hz, 3H). ^{13}C NMR (126 MHz, DMSO-d6) δ 165.8, 156.0, 154.4, 145.4, 139.0, 131.7, 130.0, 129.7, 123.8, 121.3, 116.6, 111.3, 62.2, 55.9, 52.7, 41.3, 28.3, 25.0, 24.5, 19.3, 15.4. HRMS m/z: Calcd for $C_{21}H_{26}ClN_3O_4S$ $[M+1]^+$ = 452.1411. Found $[M+1]^+$ = 452.1407.

4-(6-(3,5-Dichlorophenoxy)-5-(trifluoromethyl)pyridin-3-yl)-3-methoxy-*N*-(methylsulfonyl)benzamide (33). STEP 1: To a flask charged with **52p** (0.97 g, 3.15 mmol), 2-fluoro-5-(4,4,5,5-tetramethyl-1,3,2-dioxaborolan-2-yl)-3-(trifluoromethyl)pyridine (0.968 g, 3.15 mmol), and $Pd(PPh_3)_4$ (0.182 g, 0.157 mmol) was added 1,4-dioxane (12.59 mL) and 2 M Na_2CO_3 (7.87 mL, 15.74 mmol) and the mixture purged with nitrogen for 5 min then heated for 3 d at 90 °C affording about 20% conversion to product relative to starting aryl bromide. The reaction mixture was extracted with EtOAc and the combined organics were dried with Na_2SO_4, filtered, and dried under reduced pressure. The crude residue was purified by MPLC (50 g ultra-snap column; gradient: 0-100% EtOAc in heptane, 5% CH_2Cl_2 throughout) to afford **53** (~80% pure by LC-MS) as a colorless oil which was used without further purification. MS (ESI, positive ion) m/z: 409.1. STEP 2: To a vial charged with **53** (118 mg, 0.289 mmol), 3,5-dichlorophenol (47.1 mg, 0.289 mmol) and Cs_2CO_3 (282 mg, 0.866 mmol) was added DMSO (1155 µL) and the mixture heated at 120 °C with shaking overnight. The mixture was cooled to RT, filtered through Celite, and the filtrate dried under reduced pressure. The crude oil was

filtered through a frit, washing with MeOH and purified with reversed phase preparative LC/MS: Column: Xbridge (19 x 100 mm, C18, 10 μm); flow rate: 40 mL/min; 10 min gradient 5 – 95% CH_3CN / 0.1% TFA in H_2O. The product containing eluents were directly lyophilized to afford the title compound (31 mg, 20% yield) as a white solid. MS (ESI, positive ion) m/z: 535.1 $[M]^+$. ^1H NMR (400MHz, DMSO-d_6) δ 8.60 (d, J = 1.9 Hz, 1H), 8.42 (d, J = 1.8 Hz, 1H), 7.71 (d, J = 1.6 Hz, 1H), 7.67 (dd, J = 1.6, 7.9 Hz, 1H), 7.61 (d, J = 7.9 Hz, 1H), 7.57 (t, J = 1.9 Hz, 1H), 7.48 (d, J = 1.9 Hz, 2H), 3.90 (s, 3H), 3.40 (s, 3H). ^{13}C NMR (126 MHz, DMSO-d6) δ 165.7, 157.9, 156.1, 153.9, 151.2, 138.4, 138.3, 134.6, 133.0, 130.6, 128.7, 128.5, 125.5, 121.6, 121.3, 121.2, 111.5, 56.1, 41.3. HRMS m/z: Calcd for $C_{21}H_{15}C_{l2}F_3N_2O_5S$ $[M+1]^+$ = 535.0109. Found $[M+1]^+$ = 535.011.

4-(6-(3,5-Dichlorophenoxy)-5-(difluoromethyl)-3-pyridinyl)-3-methoxy-N-(methylsulfonyl)benzamide (34). STEP 1: To a vial charged with 2-fluoro-5-(4,4,5,5-tetramethyl-1,3,2-dioxaborolan-2-yl)nicotinaldehyde **60** (250 mg, 0.996 mmol) was added 3,5-dichlorophenol (162 mg, 0.996 mmol), Cs_2CO_3 (973 mg, 2.99 mmol) and DMF (3983 μL). The mixture was heated overnight at 50 °C affording a brown suspension. The mixture was filtered through Celite washing with MeOH and the filtrate dried under reduced pressure to afford 2-(3,5-dichlorophenoxy)-5-(4,4,5,5-tetramethyl-1,3,2-dioxaborolan-2-yl)nicotinaldehyde **61** (102 mg, 26.0% yield) as a yellow oil. MS (ESI, positive ion) m/z: 394.2 $[M+H]^+$. STEP 2: To a flask charged with **52p** (296 mg, 0.962 mmol), **61** (300 mg, 0.962 mmol), and $Pd(PPh_3)_4$ (55.6 mg, 0.048 mmol) was added 1,4-dioxane (3847 μL) and Na_2CO_3 (2M) (2405 μL, 4.81 mmol) and the mixture was heated overnight at 90 °C. The mixture was filtered through Celite and the filtrate was concentrated under reduced pressure. The crude residue was dissolved in CH_2Cl_2/MeOH and loaded onto Celite and purified by reversed phase MPLC (Isolera; 55g

Interchim (30 μm, C-18) column; ramping CH_3CN in H_2O (5- 95%, 0.1% formic acid)) to afford 4-(6-(3,5-dichlorophenoxy)-5-formylpyridin-3-yl)-3-methoxy-N-(methylsulfonyl)benzamide **62** (199 mg, 41.8% yield) as a light yellow solid. MS (ESI, positive ion) m/z: 495.0 $[M+H]^+$. ^1H NMR (400MHz, DMSO-d_6) δ 12.26 (br s, 1 H), 10.41 (s, 1 H), 8.61 (d, J = 2.5 Hz, 1 H), 8.40 (d, J = 2.5 Hz, 1 H), 7.71 (d, J = 1.6 Hz, 1 H), 7.69 - 7.65 (m, 1 H), 7.60 - 7.56 (m, 2 H), 7.56 - 7.52 (m, 2 H), 3.89 (s, 3 H), 3.39 (s, 3 H). STEP 3: To a vial charged with **62** (48 mg, 0.097 mmol) was added CH_2Cl_2 (775 μL) and the resulting suspension was cooled in an ice water bath prior to the addition of (diethylamino)sulfur trifluoride (26.9 μL, 0.203 mmol). The mixture was allowed to stir and warm to RT overnight (ice melt). The crude mixture was concentrated under reduced pressure and purified by MPLC (25g ultra snap column; ramping EtOAc in heptane (0 - 100%), 5% CH_2Cl_2 throughout)) to afford the title compound with < 50% purity (10 mg). The material was further purified with reversed phase HPLC (Gilson; ramping CH_3CN in H_2O (35-95%), 0.1% TFA throughout)) to afford the title compound (4 mg, 8% yield) as a white solid, following lyophilization. MS (ESI, positive ion) m/z: 516.9 $[M+H]^+$. ^1H NMR (500MHz ,DMSO-d_6) δ 12.24 (br s, 1 H), 8.48 (s, 1 H), 8.28 (s, 1 H), 7.70 (s, 1 H), 7.66 (dd, J = 1.4, 8.0 Hz, 1 H), 7.60 - 7.53 (m, 2 H), 7.45 (m, 2 H), 7.30 (s, 1 H), 3.89 (s, 3 H), 3.40 (s, 3 H). ^{13}C NMR (126 MHz, DMSO-d6) δ 166.4, 158.6, 158.6, 156.0, 154.3, 149.5, 137.7, 137.6, 134.5, 130.3, 128.9, 128.6, 125.2, 121.4, 121.3, 116.7, 111.4, 56.0, 41.1. Calcd for $C_{21}H_{16}Cl_2F_2N_2O_5S$ $[M+1]^+$ = 517.0203. Found $[M+1]^+$ = 517.02.

4-(5-Cyano-6-(3,5-dichlorophenoxy)-3-pyridinyl)-3-methoxy-*N*-(methylsulfonyl)benzamide (35). STEP 1: A mixture of 3-amino-5-bromo-2-fluoropyridine **63** (50 g, 261.7 mmol), bispinacolatodiborane (79.7 g, 314.1 mmol) and KOAc (77.08 g, 785.1 mmol) in 1,4-dioxane (500 mL) was degassed with nitrogen for 10 min. $PdCl_2(dppf)\cdot DCM$ (21.2 g, 26.1 mmol) was

added to the reaction mixture, which was again degassed with nitrogen for 10 min. The reaction mixture was heated at 90 °C overnight. After cooling to RT, the reaction mixture was filtered through Celite, washing with EtOAc (2 x 100 mL). The combined filtrate was concentrated under reduced pressure to afford the crude material which was purified by column chromatography (silica gel 230-400 mesh, gradient 0-10% EtOAc in hexane) to afford 2-fluoro-5-(4,4,5,5-tetramethyl-1,3,2-dioxaborolan-2-yl)pyridin-3-amine **64** (52.0 g, 84%). MS (ESI, positive ion) m/z: 239.1 $[M+1]^+$. ^{1}H NMR (300 MHz, $CDCl_3$) δ.94 (s, 2H), 7.48 (d, J = 11.0 Hz, 2H), 1.33 (s, 12H). STEP 2: A solution of **64** (46.36 g, 194 mmol), **52p** (50 g, 162.3 mmol) and K_2CO_3 (55.9 g, 405.7 mmol) in 1,4-dioxane (750 mL) and H_2O (150 mL) was degassed with nitrogen for 10 min. $Pd(PPh_3)_4$ (18.7 g, 16.23 mmol) was added and the reaction mixture was again degassed with nitrogen for 10 min. The reaction mixture was heated at 90 °C for 16 h. After cooling, the reaction mixture was concentrated under reduced pressure to afford the crude material, which was purified by column chromatography (silica gel 60-120 mesh; 15% MeOH in CH_2Cl_2) to obtain 4-(5-amino-6-fluoropyridin-3-yl)-3-methoxy-N-(methylsulfonyl)benzamide **65** (25 g, 46% yield). MS (ESI, positive ion) m/z: 340.0 $[M+1]^+$. ^{1}H NMR (300 MHz, DMSO-d_6) δ 7.63 (s, 1H), 7.61 – 7.55 (m, 1H), 7.39 (d, J = 1.9 Hz, 1H), 7.28 (dd, J = 10.7, 2.1 Hz, 1H), 7.21 (d, J = 7.8 Hz, 1H), 5.42 (s, 2H), 3.78 (s, 3H), 2.84 (s, 3H). STEP 3: Isoamylnitrite (17.3 g, 147.4 mmol) was added to a solution of **65** (25 g, 73.7 mmol) in CH_3CN (160 mL) and the reaction mixture was stirred at RT for 10 min. CuBr (21.1 g, 147.4 mmol) was added portion-wise and the reaction mixture was stirred at RT for 3 h. The reaction mixture was quenched with saturated aqueous ammonium chloride solution (100 mL) and the aqueous layer was extracted with EtOAc (3 x 500 mL). The combined organic extracts were washed with brine (250 mL), dried over anhydrous sodium sulphate and concentrated under reduced pressure to obtain the

crude product which was purified by column chromatography (silica gel 60-120 mesh, gradient 0-10% MeOH in CH_2Cl_2) to obtain 4-(5-bromo-6-fluoropyridin-3-yl)-3-methoxy-*N*-(methylsulfonyl)benzamide **66** (12.0 g, 40% yield). MS (ESI, positive ion) m/z: 402.9 $[M+1]^+$. ^{1}H NMR (400 MHz, DMSO-d_6) δ 12.3 (s, 1H), 8.49 (dd, J = 8.7, 2.0 Hz, 1H), 8.40 (s, 1H), 7.70 (s, 1H), 7.66 (d, J = 8.1 Hz, 1H), 7.59 (d, J = 7.9 Hz, 1H), 3.90 (s, 3H), 3.41 (s, 3H). STEP 4: A suspension of **66** (1.0 g, 2.48 mmol), $Zn(CN)_2$ (580 mg, 4.96 mmol), Xantphos (120 mg, 0.248 mmol) and $Pd_2(dba)_3$ (114 mg, 0.124 mmol) in DMF (10 mL) was degassed with nitrogen for 5 min. The reaction mixture was heated at 100 °C for 70 min under microwave irradiation. The reaction mixture was filtered through Celite, washing with EtOAc and concentrated under reduced pressure to obtain the crude material which was purified by column chromatography (silica gel 60-120 mesh, gradient 0-8% MeOH in CH_2Cl_2) to afford 4-(5-cyano-6-fluoropyridin-3-yl)-3-methoxy-*N*-(methylsulfonyl)benzamide **67** (545 mg, 63% yield). MS (ESI, positive ion) m/z: 350.1 $[M+1]^+$. ^{1}H NMR (400 MHz, DMSO-d_6) δ 12.30 (s, 1H), 8.79 – 8.71 (m, 2H), 7.73 – 7.64 (m, 2H), 7.61 (d, J = 7.9 Hz, 1H), 3.90 (s, 3H), 3.41 (s, 3H). STEP 5: To a vial containing 3,5-dichlorophenol (56.7 mg, 0.35 mmol) and Cs_2CO_3 (213 mg, 0.653 mmol) was added **67** (75 mg, 0.215 mmol) and DMSO (0.716 mL). The resulting mixture was shaken at 90 °C for 5 h and then filtered through a frit, washing with IPA. The IPA was removed under reduced pressure and the crude DMSO solution was purified by reversed phase preparative LC/MS: Column: Xbridge (19 x 100 mm, C18, 10 μm); flow rate: 40 mL/min; 10 min gradient 5 – 95% CH_3CN / 0.1% NH_4OH in H_2O to afford the title compound (83.6 mg, 80%). MS (ESI, positive ion) m/z: 490.0 $[M-H]^+$. ^{1}H NMR (500 MHz, DMSO-d_6) δ 8.61 (d, J = 2.30 Hz, 1H), 8.58 (d, J = 2.30 Hz, 1H), 7.69 (s, 1H), 7.64 (d, J = 7.85 Hz, 1H), 7.52 - 7.60 (m, 3H), 7.46 (d, J = 7.85 Hz, 1H), 3.86 (s,

3H), 3.09 (s, 3H). HRMS m/z: Calcd for $C_{21}H_{15}Cl_2N_3O_5S$ $[M+1]^+$ = 492.0188. Found $[M+1]^+$ = 492.0186.

4-(5-Chloro-6-(2,5-difluorophenoxy)-3-pyridinyl)-2-fluoro-5-methoxy-*N*-(methylsulfonyl)benzamide (36). STEP 1: To a solution of methyl 2-fluoro-5-hydroxybenzoate **49** (30.0 g, 176.47 mmol) in THF:H_2O (3:1, 350 mL) was added $LiOH{\cdot}H_2O$ (22.2 g, 529.41 mmol) at RT. The reaction mixture was stirred for 16 h at RT. After evaporation to remove the THF, the reaction mixture was diluted with cold water and the pH was adjusted to ~ 3 with the addition of 1.5 N aqueous HCl. The mixture was extracted with EtOAc (3 x 250 mL). The combined extracts were washed with brine (150 mL), dried over anhydrous Na_2SO_4, filtered and evaporated to afford 2-fluoro-5-hydroxybenzoic acid as an off white solid (25.1 g, 91%). MS (ESI, negative ion) m/z: 155.4 $[M-1]^-$. STEP 2: To a solution of 2-fluoro-5-hydroxybenzoic acid (5.0 g, 32.03 mmol) in $CHCl_3$ (50 mL) was added a solution of bromine (4.9 mL, 96.09 mmol) in acetic acid (50 mL) at 0° C and the mixture was stirred for 20 h at RT. The reaction was quenched with saturated sodium sulfite solution (100 mL) and extracted with EtOAc (3 x 150 mL). The combined extracts were washed with brine (200 mL), dried over anhydrous Na_2SO_4, filtered and evaporated to afford the crude product. Trituration with hexanes afforded 4-bromo-2-fluoro-5-hydroxybenzoic acid **50** as an off white solid (3.6 g, 47% yield). MS (ESI, negative ion) m/z: 235.2 $[M-1]^-$. This material was used in the next step without further purification. STEP 3: To a solution of **50** (3.5 g, 14.89 mmol) in CH_3CN (40 mL) was added K_2CO_3 (6.16 g, 44.68 mmol) and Me_2SO_4 (5.63 g, 44.68 mmol) at RT. The mixture was stirred for 5 h at 80 °C. The reaction mixture was cooled to RT, diluted with H_2O (250 mL), and extracted with EtOAc (3 x 100 mL). The combined extracts were washed with brine (100 mL), dried with anhydrous Na_2SO_4, filtered and concentrated, then purified by column chromatography (silica gel; 5%

EtOAc in pet-ether) to afford the product in <90% purity. Trituration with Et_2O (20 mL) afforded methyl 4-bromo-2-fluoro-5-methoxybenzoate as an off-white solid (1.5 g, 38% yield). MS (ESI, positive ion) m/z: 263.3 $[M+1]^+$. STEP 4: To a solution of methyl 4-bromo-2-fluoro-5-methoxybenzoate (9.0 g, 34.22 mmol) in THF:H_2O (6:1, 100 mL) was added $LiOH{\cdot}H_2O$ (4.3 g, 102.66 mmol) at RT. The solution was stirred for 16 h at RT. The THF was removed from the reaction mixture and diluted with cold water. The pH was adjusted to ~ 3 with the addition of 1.5 N aqueous HCl. The mixture was extracted with EtOAc (3 x 250 mL). The combined extracts were washed with brine (150 mL), dried over anhydrous Na_2SO_4, filtered and evaporated to afford the crude product. Trituration with hexanes afforded 4-bromo-2-fluoro-5-methoxybenzoic acid **51a** (8.01 g, 94% yield) as an off-white solid. MS (ESI, negative ion) m/z: 249.2 $[M-1]^-$. STEP 5: To a solution of **51a** (8.0 g, 32.12 mmol) in CH_2Cl_2 (100 mL) was added methanesulfonamide (3.66 g, 38.55 mmol), DMAP (5.88 g, 48.19 mmol) and EDC·HCl (9.23 g, 48.19 mmol) and the mixture was stirred for 48 h at RT. The reaction was quenched with 1.5 N aqueous HCl (150 mL) and extracted with CH_2Cl_2 (3 x 250 mL). The combined extracts were washed with brine (150 mL), dried over anhydrous Na_2SO_4, filtered and evaporated to afford the crude product. Trituration with Et_2O:hexanes (2:8, 100 mL) afforded 4-bromo-2-fluoro-5-methoxy-*N*-(methylsulfonyl)benzamide **52a** as an off-white solid (8.5 g, 81% yield). MS (ESI, negative ion) m/z: 324.2 $[M-1]^-$. STEP 6: To a flask charged with **52a** (5.00 g, 15.33 mmol), 3-chloro-2-fluoro-5-(4,4,5,5-tetramethyl-1,3,2-dioxaborolan-2-yl)pyridine (3.95 g, 15.33 mmol), and $Pd(PPh_3)_4$ (0.886 g, 0.767 mmol) was added 1,4-dioxane (61.3 mL) and 2 M Na_2CO_3 (38.3 mL, 77 mmol). The mixture was purged with nitrogen then heated to 90 °C overnight, affording ~25% conversion to product with starting material remaining. To the mixture was added additional 3-chloro-2-fluoro-5-(4,4,5,5-tetramethyl-1,3,2-dioxaborolan-2-yl)pyridine (2 g, 7.78

mmol) and $Pd(PPh_3)_4$ (0.886 g, 0.767 mmol) and the mixture heated to 130 °C for 16 h affording complete conversion to desired product. The suspension was cooled in an ice water bath and brought to pH < 2 with the addition of 6 N HCl, affording a precipitate which was collected by vacuum filtration, washed with water, and dried under a vacuum/nitrogen sweep. The resulting solid was triturated with MeOH/H_2O (1:1) and washed with H_2O, to afford 4-(5-chloro-6-fluoropyridin-3-yl)-2-fluoro-5-methoxy-N-(methylsulfonyl)benzamide **54** (5.26 g, 91% yield) as a light yellow solid. MS (ESI, positive ion) m/z: 376.8 $[M+1]^+$. ^{1}H NMR (400MHz, DMSO-d_6) δ 12.36 (br s, 1H), 8.38 (m, 2H), 7.40 (m, 2H), 3.83 (s, 3H), 3.13 (s, 3H). STEP 7: To a resealable screw cap vial containing **54** (1 g, 2.65 mmol) was added DMSO (8.85 mL), Cs_2CO_3 (2.59 g, 7.96 mmol), and 2,5-difluorophenol (0.414 g, 3.19 mmol). The reaction mixture was heated at 90 °C with shaking overnight. After cooling to RT, the reaction mixture was poured into 15 mL of H_2O and was extracted with CH_2Cl_2 (3 x 20 mL). The combined organic layers were dried over sodium sulfate, filtered, and concentrated in vacuo. The crude material was absorbed onto a plug of silica gel and purified by MPLC (Redi-Sep pre-packed silica gel column (40 g), gradient: 0-100% EtOAc in hexane), to provide the title compound < 90% pure. This material was further purified by MPLC (Redi-Sep pre-packed silica gel column (40 g), gradient of 0-10% MeOH in CH_2Cl_2) to afford the pure title compound (610 mg, 47% yield) as a white solid. MS (ESI, positive ion) m/z: 487.9 $[M+1]^+$. ^{1}H NMR (400 MHz, DMSO-d6) δ 8.32 (d, J = 2.18 Hz, 1H), 8.27 (d, J = 2.07 Hz, 1H), 7.44 - 7.55 (m, 3H), 7.36 (d, J = 5.80 Hz, 1H), 7.17 - 7.28 (m, 1H), 3.86 (s, 3H), 3.40 (s, 3H). ^{13}C NMR (126 MHz, DMSO-d6) δ 163.4, 158.0, 156.5, 153.6, 152.1, 150.8, 145.4, 140.7, 140.3, 128.9, 121.5, 118.2, 117.6, 116.3, 116.2, 113.6, 112.6, 112.2, 56.5, 41.3. HRMS m/z: Calcd for $C_{20}H_{14}ClF_3N_2O_5S$ $[M+1]^+$ = 487.0342. Found $[M+1]^+$ = 487.0341.

4-(5-Chloro-6-((1-methylcyclopropyl)methoxy)-3-pyridinyl)-2-fluoro-5-methoxy-*N*-(methylsulfonyl)benzamide (37). Using General Procedure F, reaction of **54** and (1-methylcyclopropyl)methanol at 120 ºC afforded the title compound (20 mg, 18% yield) as an off-white solid. MS (ESI, negative ion) m/z: 441.0 $[M-1]^-$. ^{1}H NMR (500 MHz, DMSO-d_6) δ 8.25 (d, J = 2.08 Hz, 1H), 8.06 (d, J = 2.08 Hz, 1H), 7.34 (d, J = 6.10 Hz, 1H), 7.26 (d, J = 10.70 Hz, 1H), 4.20 (s, 2H), 3.80 (s, 3H), 3.01 (s, 3H), 1.20 (s, 3H), 0.51 - 0.63 (m, 2H), 0.36 - 0.46 (m, 2H). ^{13}C NMR (126 MHz, DMSO-d6) δ 163.3, 158.1, 153.7, 152.0, 145.1, 139.2, 129.9, 125.9, 120.9,117.9, 116.4, 112.6, 74.2, 56.5, 41.3, 20.7, 15.4, 11.0. HRMS m/z: Calcd for $C_{19}H_{20}ClFN_2O_5S$ $[M+1]^+$ = 443.0844. Found $[M+1]^+$ = 443.0838.

4-(5-Chloro-6-(cyclobutyloxy)-3-pyridinyl)-2-fluoro-5-methoxy-N-(methylsulfonyl)benzamide (38). Using General Procedure F, reaction of **54** and cyclobutanol at 120 ºC afforded the title compound (35 mg, 33% yield) as an off-white solid. MS (ESI, negative ion) m/z: 427.0 $[M-1]^-$. ^{1}H NMR (500 MHz, DMSO-d_6) δ 8.34 (d, J = 2.08 Hz, 1H), 8.14 (d, J = 2.08 Hz, 1H), 7.42 (d, J = 6.03 Hz, 1H), 7.34 (d, J = 10.70 Hz, 1H), 5.32 (quin, J = 7.35 Hz, 1H), 3.88 (s, 3H), 3.10 (s, 3H), 2.50 - 2.56 (m, 2H), 2.15 - 2.25 (m, 2H), 1.90 (q, J = 10.10 Hz, 1H), 1.70 - 1.80 (m, 1H). ^{13}C NMR (126 MHz, DMSO-d6) δ 163.3, 157.1, 153.7, 152.1, 145.3, 139.2,129.9, 126.1, 121.0, 117.9, 116.3, 112.5, 70.6, 56.5, 41.3, 30.3, 13.0. HRMS m/z: Calcd for $C_{18}H_{18}ClFN_2O_5S$ $[M+Na]^+$ = 451.0501. Found $[M+Na]^+$ = 451.0490.

General Procedure A for the parallel S_NAr reaction of alcohols and 45: Resealable screw cap reaction vials (20 mL) were placed in a reaction block and each vial was charged with **45**, (300 mg, 1.054 mmol), alcohol (1.159 mmol) and Cs_2CO_3 (1030 mg, 3.16 mmol). DMSO (4 mL) was added to each vial and the vials were sealed. The block was heated at 130 °C with shaking on a J-KEM Scientific MaxQ 2000 heater-shaker overnight. After cooling to RT, the

resulting suspensions were poured into a mixture of NH_4Cl (aq) and ice. The resulting slurries were brought to pH < 2 by the addition of 6N HCl, affording precipitates which were collected by vacuum filtration and washed with water, then dried overnight under vacuum to afford the pure products.

General Procedure B for the parallel synthesis of acyl sulfonamides 7a-t from 3,4-dichlorophenyl-containing carboxylic acids: Resealable screw cap reaction vials (2 dram) were placed in a reaction block and each vial was charged with carboxylic acid (0.526 mmol), methanesulfonamide (0.060 g, 0.631 mmol), DMAP (0.141 g, 1.157 mmol), and EDC·HCl (0.202 g, 1.052 mmol). CH_2Cl_2 (2 mL) and DMF (1 mL) were added to each vial. The vials were sealed and the block was shaken on a J-KEM Scientific MaxQ 2000 heater-shaker overnight at RT. The mixtures were filtered through an Isolute filtration column, washing with CH_2Cl_2 and MeOH. After evaporation of the volatile solvents, minimal DMSO was added and the solutions were filtered through a Nalgene PTFE 0.2 μM filter, then purified by high throughput parallel purification with reversed phase preparative LC/MS: Waters auto-purification system; liquid transfer system: Tecan; drying system: Genevac; prep. Column: Xbridge (19 x 100 mm, C18, 10 μm); flow rate: 40 mL/min; general gradient: 5 – 95% B, 0.1% additive in both A and B; 10 min gradient; Mobile Phase A: H_2O, Mobile Phase B, CH_3CN; Additive: TFA or NH_4OH.

General Procedure C for the parallel S_NAr of alcohols and fluoride 24. Resealable screw cap reaction vials (2 dram) were placed in a reaction block and each vial was charged with alcohol (0.418 mmol), Cs_2CO_3 (216 mg, 0.664 mmol), and **24** (100 mg, 0.265 mmol). DMSO (1 mL) was added to each vial and the vials were capped. The block was heated at 90 ºC (phenols) or 120 ºC (aliphatic alcohols) with shaking on a J-KEM Scientific MaxQ 2000 heater-shaker

overnight. After cooling, the mixtures were filtered through an Isolute filtration column, washing with CH_2Cl_2 and MeOH. After evaporation of the volatile solvents, minimal DMSO was added and the solutions were filtered through a Nalgene PTFE 0.2 μM filter, then purified by high throughput parallel purification with reversed phase preparative LC/MS: Waters auto-purification system; liquid transfer system: Tecan; drying system: Genevac; prep. Column: Xbridge (19 x 100 mm, C18, 10 μm); flow rate: 40 mL/min; general gradient: 5 – 95% B, 0.1% additive in both A and B; 10 min gradient; Mobile Phase A: H_2O, Mobile Phase B, CH_3CN; Additive: TFA or NH_4OH.to provide the pure products as solids upon concentration in vacuo.

General Procedure D for the parallel S_NAr of thiols and fluoride 24. Resealable screw cap reaction vials were placed in a reaction block and each vial was charged with thiol (0.300 mmol), Cs_2CO_3 (0.143 g, 0.440 mmol), and **24** (0.079 g, 0.2 mmol). DMSO (1.0 mL) was added to each vial and the vials were sealed. The block was heated at 100 °C with shaking on a J-KEM Scientific MaxQ 2000 heater-shaker overnight. After cooling, the mixtures were filtered through an Isolute filtration column, washing with CH_2Cl_2 and MeOH. After evaporation of the volatile solvents, minimal DMSO was added and the solutions were filtered through a Nalgene PTFE 0.2 μM filter, then purified by high throughput parallel purification with reversed phase preparative LC/MS: Waters auto-purification system; liquid transfer system: Tecan; drying system: Genevac; prep. Column: Xbridge (19 x 100 mm, C18, 10 μm); flow rate: 40 mL/min; general gradient: 5 – 95% B, 0.1% additive in both A and B; 10 min gradient; Mobile Phase A: H_2O, Mobile Phase B, CH_3CN; Additive: TFA or NH_4OH to afford the products as solids.

General Procedure E for the parallel S_NAr of amines and fluoride 24. Resealable screw cap vials (2 dram) were placed in a reaction block and charged with **24** (100 mg, 0.278 mmol) and amine (0.334 mmol). DMSO (1.0 mL) and NEt_3 (116 μL, 0.834 mmol) were added and the vials

were sealed and heated at 90 °C with shaking on a J-KEM Scientific MaxQ 2000 heater-shaker overnight. After cooling, the solutions were filtered through a Nalgene PTFE 0.2 μM filter, then then purified by high throughput parallel purification with reversed phase preparative LC/MS: Waters auto-purification system; liquid transfer system: Tecan; drying system: Genevac; prep. Column: Xbridge (19 x 100 mm, C18, 10 μm); flow rate: 40 mL/min; general gradient: 5 – 95% B, 0.1% additive in both A and B; 10 min gradient; Mobile Phase A: H_2O, Mobile Phase B, CH_3CN; Additive: TFA or NH_4OH. to afford the products as solids.

General Procedure F for the parallel S_NAr of alcohols to fluoride 54. Resealable screw cap reaction vials (2 dram) were placed in a reaction block and each vial was charged with alcohol (0.418 mmol), Cs_2CO_3 (216 mg, 0.664 mmol), and **54** (100 mg, 0.265 mmol). DMSO (1 mL) was added to each vial and the vials were capped. The block was heated at 90 ºC (phenols) or 120 ºC (aliphatic alcohols) with shaking on a J-KEM Scientific MaxQ 2000 heater-shaker overnight. After cooling, the mixtures were filtered through an Isolute filtration column, washing with CH_2Cl_2 and MeOH. After evaporation of the volatile solvents, minimal DMSO was added and the solutions were filtered through a Nalgene PTFE 0.2 μM filter, then purified by high throughput parallel purification with reversed phase preparative LC/MS: Waters auto-purification system; liquid transfer system: Tecan; drying system: Genevac; prep. Column: Xbridge (19 x 100 mm, C18, 10 μm); flow rate: 40 mL/min; general gradient: 5 – 95% B, 0.1% additive in both A and B; 10 min gradient; Mobile Phase A: H_2O, Mobile Phase B, CH_3CN; Additive: TFA or NH_4OH to provide the pure products as solids upon concentration in vacuo.

Human stable cell lines. Human $Na_V1.1$ (HEK293), 1.2 (CHO), 1.3(CHO), 1.4(HEK293), 1.5(HEK293), 1.6(HEK293), and 1.7(HEK293 stable cell lines were purchase from Eurofins

Pharma Bioanalytics Services US Inc., St. Charles, MO. A tetracycline-inducible human $Na_V1.8$ CHO cell line was generated internally.

Rodent stable cell line development. Rodent $Na_V1.7$ sequences were sub-cloned into the antibiotic selection vector pSLX240h, linearized and stably transfected using Lipofectamine LTX (Life Technologies, Grand Island, NY) into HEK293 (for mouse $Na_V1.7$) or HEK293T (for rat $Na_V1.7$) cells grown in DMEM/F12,+10%Serum,+1X P/S/G,+1X NEAA,+15 mM HEPES. Following 48-72 h of transfection, media containing 80 μg/mL hygromycin was added and selection was continued for 24-30 d. When the stable pools formed good-sized colonies, individual colonies were picked into 96 well plates, expanded, and expression was confirmed by electrophysiology testing and Western blot.

PatchXpress 7000A electrophysiology. Sodium currents were recorded in whole cell voltage clamp mode with the PatchXpress automated electrophysiology system (Molecular Devices, LLC, Sunnyvale, CA). Adherent cells were isolated from tissue culture flasks using trypsin-EDTA treatment for 2-3 min and then incubated in complete culture medium containing 10% fetal bovine serum for at least 15 min prior to resuspension in external solution consisting of 70 mM NaCl, 140 mM D-Mannitol, 5 mM KCl, 11 mM Glucose, 10 mM HEPES, 2 mM $CaCl_2$, 1 mM $MgCl_2$, pH 7.4 with NaOH. Internal solution consisted of 62.5 mM CsCl, 75 mM CsF, 10 HEPES, 5 mM EGTA, 2.5 mM $MgCl_2$, pH 7.25 with CsOH. Cells were voltage clamped at room temperature at a holding potential of -125 mV with test potentials to -10 mV ($Na_V1.7$) or -20 mV ($hNa_V1.5$). Compound effects were measured on a partially inactivated state of sodium channels. For human, mouse, and rat $Na_V1.7$, cells were clamped to a holding potential yielding 20-50% inactivation. To elicit sodium current, channels were activated by pulsing to -10 mV for 15 msec. This voltage protocol was repeated at a rate of 0.1 Hz throughout the experiment. For

human $Na_V1.5$, cells were held at a holding potential of -50 mV. To elicit sodium currents the voltage was changed to -120 mV for a period of 50 msec before a test pulse to -20 mV of 20 msec duration. These voltage protocols were repeated at a rate of 0.1 Hz throughout the experiment. A single concentration of test compound was applied to cells for 3-5 min. Peak sodium current was measured at the end of the compound addition period to determine percent inhibition. Cells were used for additional compound testing if currents recovered to >80% of starting values following compound washout. IC_{50} values were calculated by pooling single point determinations from three to five cells at different compound concentrations and fitting the resulting dataset with a Hill (4-parameter logistic) fit in DataXpress 2.0 software.

Manual patch-clamp electrophysiology. Cells were voltage clamped using the whole cell patch clamp configuration at room temperature. Pipette resistances were between 1.5 and 2.0 MΩ. Whole cell capacitance was uncompensated. Currents were digitized at 50 kHz and filtered (4-pole Bessel) at 10 kHz using pClamp10.2. Cells were lifted off the culture dish and positioned directly in front of a micropipette connected to a solution exchange manifold for compound perfusion. To record from partially inactivated channels, cells were held at -140 mV initially and then switched to a voltage that yielded ~20% channel inactivation. 20 ms pulses to -10 mV (0 mV for $Na_V1.8$) were delivered every 10 seconds and peak inward currents were recorded before and after compound addition. For $hNa_V1.8$ channel recordings, tetrodotoxin (TTX, 0.5 uM) was added to inhibit endogenous TTX-sensitive voltage-gated sodium channels and record only $Na_V1.8$-mediated TTX-resistant currents. To record from fully non-inactivated (resting/closed state) channels, cells were held at -140 mV for the entire duration of the experiment. 10 ms pulses were delivered every 10 seconds and peak inward currents were recorded before and after compound addition. External solution consisted of: 140 mM NaCl,

5.0 mM KCl, 2.0 mM $CaCl_2$, 1.0 mM $MgCl_2$, 10 mM HEPES, and 11 mM Glucose, pH 7.4 by NaOH. Internal solution consisted of: 62.5 mM CsCl, 75 mM CsF, 2.5 mM $MgCl_2$, 5 mM EGTA, and 10 mM HEPES, pH 7.25 by CsOH. Escalating compound concentrations were analyzed on the same cell and IC_{50} values were calculated by fitting the resulting dataset with a Hill (4-parameter logistic) fit in Origin Pro 8 software.

DRG Neuron Isolation and Manual Patch Clamp Electrophysiology. All in vivo procedures for DRG neuron isolation were approved by the Institutional Animal Care and Use Committee at Amgen (Thousand Oaks, CA). Adult male and female C57BL/6 mice (Charles River Laboratories, San Diego, CA) were euthanized with CO_2 followed by decapitation. DRG from cervical, thoracic and lumbar regions were removed, placed in Ca^{2+}- and Mg^{2+}-free Hanks' Balanced Salt Solution (Invitrogen, Carlsbad, CA), and trimmed of attached fibers under a dissecting microscope. DRG were sequentially digested at 37 °C with papain (20 U/ml, Worthington Biochemical Corporation, Lakewood, NJ) and L-cysteine (25 μM) in Ca^{2+} and $Mg2^{+}$-free Hanks' (pH 7.4) for 20-30 min and then with collagenase type 2 (0.9% w/v, Worthington Biochemical Corporation) for 20-30 min. Digestions were quenched in Neurobasal Medium (Fisher Thermo Scientific) and cells were triturated with a fire-polished Pasteur pipette prior to plating on Poly-D-Lysine-coated glass coverslips (Cole-Parmer, Vernon Hills, IL). Cells were maintained in a humidified incubator at 32 °C with 5% CO_2 for 5-7 days in Neurobasal Medium with 2% B-27 Supplement, serum free (Fisher Thermo Scientific) to increase the expression of tetrodotoxin-sensitive sodium channel currents. DRG neurons were voltage clamped using the whole-cell patch clamp configuration at room temperature using an Axopatch MultiClamp 700 B amplifier and DIGIDATA 1322A with pCLAMP software (Molecular Devices, Sunnyvale, CA). Pipettes, pulled from borosilicate glass capillaries (World Precision

Instruments, Sarasota, FL), had resistances between 1.0 and 3.0 MΩ. Currents were digitized at 50 kHz and filtered (4-pole Bessel) at 10 kHz. Cells were lifted off the culture dish and positioned directly in front of a micropipette connected to a solution exchange manifold for compound perfusion. Cells were held at -140 mV or a voltage yielding approximately 20% inactivation and depolarized to -10 mV for 40 msec every 10 seconds. Tetrodotoxin (TTX, Sigma) was used following compound addition to block any residual TTX-sensitive sodium currents. Pipette solution contained (in mM): 62.5 CsCl, 75 CsF, 2.5 $MgCl_2$, 5 EGTA, and 10 HEPES, pH 7.25 by CsOH. Bath solution contained (in mM): 70 NaCl, 5.0 KCl, 2.0 $CaCl_2$, 1.0 $MgCl_2$, 10 HEPES, and 11 glucose, 140 mannitol, pH 7.4 by NaOH. Data were analyzed with Clampfit and Origin Pro8 (OriginLab Corp, Northampton, MA).

IonWorks Quattro electrophysiology. Sodium currents were recorded in population patch-clamp mode with the IonWorks® Quattro automated electrophysiology system (Molecular Devices, LLC, Sunnyvale, CA). This system utilizes perforated patch-clamp technology to gain electrical access to cells. External saline consisted of (in mM): NaCl 140, KCl 5, $CaCl_2$ 2 $MgCl_2$ 1, HEPES 10 and glucose 11; pH 7.4 with N-methyl-D-glucamine; 320 mOsmol. Internal solution for hNav1.5 and hNav1.7 consisted of (in mM): of KCl 70, KF 70, $MgCl_2$ 0.25, HEDTA 5 and HEPES 10; pH 7.25 with *N*-methyl-*D*-glucamine; 300 mOsmol. Cells were voltage clamped to -110 mV for three seconds (Nav1.7) or half a second (Nav1.5) and sodium currents were elicited by a train of 26 depolarizations of 150 msec duration at 5 Hz to -20 mV at a frequency of 5 Hz. Cells were then left unclamped for a period of 3 to 8 minutes while a single concentration of test compound was added. Following this compound incubation period, cells were then reclamped to -110 mV for three seconds (Nav1.7) or half a second (Nav1.5) to recover unbound channels and put through the same 26 pulse voltage protocol as above. Peak inward

current during the 26th pulse to -20 mV in the presence of compound was divided by the peak inward current evoked by the 26th pulse to -20 mV or 0 mV in the absence of compound to determine percent inhibition. Concentration-response curves of percent inhibition as a function of concentration were generated to calculate IC_{50} values. For IC_{50} determination, data was fitted to a 4-parameter equation (y = A + ((B-A)/(1 + ((x/C)^D))), where A is the minimum y (POC) value, B is the maximum y (POC), C is the x (compound concentration) at the point of inflection and D is the slope factor). Non-linear regression curve-fitting was performed using Screener (Genedata AG, Basel, Switzerland) data analysis software.

Human $Na_V1.7$ ^{3}H-Radioligand Binding Assay. Human $Na_V1.7$-HEK293 membranes were prepared at 4 ^{o} C. Cell pellets were suspended in membrane buffer (50 mM Tris HCl, pH 7.4 (Lonza, Walkersville, MD), 1% v/v protease inhibitor cocktail (complete™ ULTRA Tablets, Mini, EDTA-free, Roche Applied Science, Mannheim, Germany)). Cells were then lysed using a glass dounce homogenizer and centrifuged at 200 x g for 15 min. The supernatant was collected and spun at 10000 x g for 50 min in a floor model centrifuge. Pelleted membranes were re-suspended in membrane buffer and the mixture was further refined by homogenization in a small glass dounce homogenizer followed by passage through a 26 gauge needle. The protein concentration of the finished membrane preparation was determined using the bicinchoninic acid (BCA) method (Pierce Chemical, Rockford, IL). For competition binding assays, test compounds were pre-incubated with 2 µg of human $Na_V1.7$-HEK293 membrane in 200 µL of binding buffer (100 mM NaCl, 20 mM Tris HCl, pH7.4) for 30 min at RT. Next, 100 µL of binding buffer containing 0.75 nM tritiated-radioligand was added (final concentration of 0.25 nM; approximate K_d) and the reaction was incubated for an additional hour at RT. Meanwhile, filter plates (UniFilter-96 GF/C, white 96-well Barex Microplates with 1.2 µm

poresize , Perkin Elmer, Downers Grove, IL) were soaked with 40 µL per well of 0.5% polyethylenimine (PEI) (Sigma-Aldrich, St Louis, MO) for 1 h before washing 3 times with ice cold wash buffer (100 mM NaCl, 20 mM Tris HCl, pH 7.4, 0.1 % BSA (Sigma-Aldrich)). The binding reaction was then added to the filter plates and the plates were washed 3 times to remove unbound radioligand. The filter plates were air-dried for 2 - 4 h before adding 40 µL per well of scintillation cocktail (Microscint-20™, Perkin Elmer). Filter-bound radioactivity was measured on a luminescence plate reader (MicroBeta® JET, Perkin Elmer). Compound potencies (IC_{50}) were determined using Screener (Genedata AG, Basel, Switzerland) analysis software from 10 concentration points that consisted of 2 replicates per concentration point. The amount of signal generated in the presence of compounds versus that in the presence of DMSO vehicle alone (high control) and excess cold ligand (low control) was calculated using the formula: % control (POC) = (compound – average low)/(average high – average low)*100. Potency data was fitted to a 4-parameter equation (y = A + ((B-A)/(1 + ((x/C)^D))), where A is the minimum y (POC) value, B is the maximum y (POC), C is the x (compound concentration) at the point of inflection and D is the slope factor).

Solubility Determination. Solubilities in PBS and FaSSIF were determined according to an automated procedure.[27]

Transport across MDR1-LLC-PK1 Cells. Transport studies to determine apparent permeability and efflux ratios [Efflux ratio = $Papp_{,B\rightarrow A}/Papp_{,A\rightarrow B}$] were performed in MDR1-transfected or BCRP-transfected LLC-PK1 cells with compounds tested at 5 µM in the presence of 0.1% BSA as described.[28]

CYP Inhibition IC50. Inhibition of CYP3A4 , 2D6, and 2C9 was determined as described.[18]

Rat and Human Liver Microsomal Assays. Test compounds (1 μM) were incubated at 37 °C in phosphate buffer (66.7 mM, pH 7.4) with pooled human or rat liver microsomes (0.25 mg/mL protein) and 1 mM NADPH. After 1, 5, 10, 20, 30 and 40 minutes, the reaction was stopped by the addition of acetonitrile containing 0.5% formic acid and internal standard. The quenched samples were centrifuged at 1650 g for 20 min. The supernatants were analyzed directly for unchanged test compound using liquid chromatography and tandem mass spectrometric detection (LC-MS/MS).

Plasma Protein Binding. The protein binding of compounds in mouse and rat plasma was determined by ultracentrifugation. In brief, compound in DMSO was added to 1 mL of pooled, mixed-gender mouse or rat plasma (BioreclamationIVT, Baltimore, MD) to achieve a final concentration of 5 μM. A 500 μL aliquot of the spiked plasma sample was transferred to ultracentrifuge tubes and equilibrated in an Optima Max-XP ultracentrifuge (Beckman Coulter, Jersey City, NJ) for 45 min at 37 °C followed by centrifugation at 627,000 rcf for 3 h at 37 °C. Prior to centrifugation a portion of the spiked plasma samples were transferred to separate tubes that were stored at 4 °C (to determine total plasma concentration) or 37 °C (to determine plasma stability) for the duration of the centrifugation step. After ultracentrifugation, 100 μL of each supernatant was added to an equal volume of blank plasma. An aliquot of the plasma samples for total plasma concentration and stability determination was added to an equal volume of 0.2 μm filtered plasma water. Protein precipitation was achieved by adding 2 volumes (v/v) of ice cold acetonitrile containing 1 μM tolbutamide as an internal standard and centrifuging the samples for 10 min at 3000 rpm. A portion of the supernatant was transferred for liquid chromatography-tandem mass spectrometry (LC-MS/MS) analysis. LC-MS/MS analysis of compound was performed on an API4000 triple quadrupole mass spectrometer (Applied

Biosystems, Foster City, CA) using negative electrospray ionization and coupled to a Shimadzu UFLC-30AD-Nexera sample delivery system (Shimadzu, Columbia, MD). Peak separation incorporated a Kinetex C18 50 x 2.1 mm (5 um) chromatographic column (Phenomenex, Torrance, CA) and rapid gradient conditions (total run time 1 minute) using 0.1% formic acid in water and 0.1% formic acid in acetonitrile as the mobile phase system. The analyte compound and internal standard tolbutamide were monitored using multiple reaction monitoring transitions of 485.1 / 364.1 (Q1/Q3) and 268.9 / 169.7, respectively. Common LC/MS-MS parameters included the source temperature (600 °C), curtain gas (35 arbitrary units), CAD gas (10 arbitrary units), and source gases 1 and gas 2 (25 and 0 arbitrary units, respectively). Data analysis was evaluated using Analyst (version 1.6.1; Applied Biosystems, Foster City, CA). Test article concentrations were estimated by calculating peak areas in unknown samples relative to those obtained from standard curves with synthetic standards (linear range: 1 – 15000 ng/mL). The fraction unbound was calculated as the ratio of the concentration of the compound in the supernatant from centrifuged samples as compared to the concentration of the compound in the samples stored at 4 °C for total concentration determination.

Rat Pharmacokinetic Studies. All pharmacokinetic procedures described in this manuscript were approved by the Institutional Animal Care and Use Committee at Amgen (Thousand Oaks, CA). In order to characterize the pharmacokinetic properties of compound**s**, jugular vein catheterized male rats (250 – 350 g, 8 – 10 weeks old; Harlan, Cambridgeshire, UK) were dosed intravenously (1 mg/kg, DMSO solution) or orally (10 mg/kg, 1.0% Tween 80, 2.0% hydroxypropylmethylcellulose, 97% water, pH 8.5 with NaOH). Serial blood samples were collected via the jugular vein catheter into K_2-EDTA collection tubes and immediately placed on ice, followed by centrifugation (4 °C, 10 min, 13000 rpm) in order to obtain plasma. Protein

precipitation and LC-MS/MS analysis of the in vivo samples was performed in a similar manner as described under the plasma protein binding section except for the volume of acetonitrile used to quench the protein samples and the internal standard used, which were 5 volumes (v/v) and 0.1 μg/mL verapamil, respectively. The LC-MS/MS multiple reaction monitoring transition used for verapamil was 307.1 / 160.8 (Q1/Q3). Estimation of pharmacokinetic parameters was performed through noncompartmental analysis (Phoenix64, Cetara, Princeton, NJ).

Open Field Locomotor Activity in Mice. All procedures were approved and carried out in accordance with Amgen Inc.'s Institutional Animal Care and Use Committee. Subjects were C57Bl/6 male mice (Charles River Labs, Kingston, NY) aged between 9-10 weeks and housed 1-4 per cage with *ad libitum* access to food and water. Animals were kept on a 12/12 h light/dark cycle with lights on at 6:30 a.m. Following arrival from the vendor, mice were allowed to acclimate to the animal facility for 1 week prior to the start of the experiment. On the day of testing, animals were orally administered either **36** (30, 100, or 300 mg/kg body weight) or a vehicle control formulation (30% Hydroxypropyl beta-cyclodetrin, 70% H_2O, pH10) between the hours of 7:00 a.m. and 5:00 p.m. Four hours following test article treatment, animals were placed into dimly-lit (15-20 Lux) open-field chambers (16" x 16", Kinder Scientific, San Diego, CA) and behavior was monitored over a 60 min period during which movement parameters were measured in an automated manner via infrared photo beam breaks. Data was analyzed statistically via GraphPad Prism 5 software (GraphPad Software Inc., La Jolla, CA) using a one-way ANOVA to assess the overall test article treatment effect and followed by Dunnett's multiple comparison post-hoc tests.

Histamine-Induced Scratching in Mice. All procedures were approved and carried out in accordance with Amgen Inc.'s Institutional Animal Care and Use Committee. Subjects were

C57Bl/6 male mice (Charles River Labs, Kingston, NY) aged between 9-10 weeks and housed 1-4 per cage with *ad libitum* access to food and water. Animals were kept on a 12/12 h light/dark cycle with lights on at 6:30 a.m. Following arrival from the vendor, mice were allowed to acclimate to the animal facility for 1 week prior to the start of the experiment. One day prior to behavioral testing, mice were anesthetized under 3% isoflurane and the area at the nape of the neck was shaved. Immediately afterward, mice were transported to the testing room and acclimated to individual sound-attenuated chambers (12"l X 9.5"w X 8.25"h, Med Associates VFC-008, NIR-022MD, St. Albans, VT) for 15-20 min. Testing was performed the following day between the hours of 8:00 am and 3:00 pm. Four hours prior to histamine treatment, mice were orally administered either **36** (30, 100, or 300 mg/kg body weight), a vehicle control formulation (30% Hydroxypropyl beta-cyclodextrin, 70% H_2O, pH10), or the antihistamine Diphenhydramine (30 mg/kg in phosphate-buffered saline, Sigma D3630) which served as a positive control. Histamine dichloride (8.15 mM in a volume of 100 µL, Sigma Aldrich H7250) was injected intradermally to the shaved area, mice were placed into the sound-attenuated testing chambers, and behavior was recorded on digital video files for a period of 15 min. Video recordings were later reviewed, and individual scratching bouts scored, by trained experimenters blinded to test article treatment. A scratching bout was defined as a rapid head tilt accompanied by a hind paw directed at the site of intradermal injection. Termination of a scratching bout was deemed to have occurred when the hind paw was placed back on the chamber floor or into the animal's mouth. Data was analyzed statistically via GraphPad Prism 5 software (GraphPad Software Inc., La Jolla, CA) using a one-way ANOVA to assess the overall test article treatment effect and followed by Dunnett's multiple comparison post-hoc tests.

Ligand Docking. Docking analyses were performed with Schrodinger's Glide Dock (Schrodinger LLC) with a SP (Standard Precision) option and the crystal structure of the published human Nav1.7-VSD4-NavAb complex (5EK0).

ASSOCIATED CONTENT

Supporting Information

For **36**: Copies of ^{1}H and ^{13}C NMR spectra; Mouse DRG dose-response curves; PD and PK data for dose-response studies in mouse Histamine-Induced Scratching and OFA. The Supporting Information is available free of charge on the ACS Publications website at DOI: brief description (file type, i.e., PDF)

AUTHOR INFORMATION

Corresponding Author

* Phone: 617-444-5189. E-mail: edimauro@amgen.com

Present Addresses

[‡]Author's current address is as follows:

For S.A.: Department of Applied Discovery Research, Sanofi-Genzyme, 49 New York Ave., Framingham, MA. 01701, United States.

For E.F.B.: International Burch University, Faculty of Engineering and Information Technologies, Department of Genetics and Bioengineering. Francuske Revolucije bb, Ilidža, 71000, Sarajevo, Bosnia and Herzegovina.

For R.F.: NeuroRx Consulting, 854 Massachusetts Avenue, Unit 3. Cambridge, MA. 02139 United States.

For H.G.: Merck & Co., Inc., 33 Avenue Louis Pasteur, Boston, MA. 02115, United States.

For H.H.: Center for Drug Discovery, Department of Pathology and Immunology, Baylor College of Medicine, One Baylor Plaza, Houston, TX. 77030, Unites States.

For D.O.: Novartis Institute of Biomedical Research Inc., 250 Mass Ave. Cambridge, MA. 02139, Unites States.

Author Contributions

All authors have contributed and have given approval to the final version of the manuscript.

Notes

The authors declare no competing financial interest.

ACKNOWLDGMENTS

We thank the following people for their contributions: Jiali Hu for contributions to cell line development; Larry Miller and Grace Bi for high throughput purification; Steven Hollis for the high throughput ^{1}H NMR and ^{13}C NMR characterization of compounds; Iain Campuzano for the generation of HRMS characterization data; Christopher Ilch and Kimberly Nye for assisting in the collection of mouse behavioral data; Loren Berry, Brett Janosky and Liyue Huang for the determination of in vitro ADME parameters.

ABBREVIATIONS

BSEP, bile salt export pump: hERG, human ether-a-go-go related gene; μW, microwave; CL, clearance; PPB, plasma protein binding; DRG, dorsal root ganglion neuron; TTX-S, tetrodotoxin-sensitive; LipE, lipophilic efficiency; AUC_{inf}, area under the concentration time curve from 0 h to infinity; Vd, volume of distribution; F, bioavailability; OATP, organic anion-transporting polypeptide; SCN9A, sodium channel protein type 9 subunit alpha; IWQ, IonWorks Quattro; PX, Patch-Xpress; EDC *N*-(3-dimethylaminopropyl)-*N*′-ethylcarbodiimide; DAST,

diethylaminosulfur trifluoride; VSD4, voltage-sensor domain 4; ABCG2, ATP-binding cassette sub-family G member 2

REFERENCES

(1) Hille B. *Ion Channels of Excitable Membranes*, 3rd ed.; Sinauer Associates, Inc.: Sunderland MA, 2001.

(2) (a) Goldin, A. L, Resurgence of sodium channel research. *Ann. Rev. Physiol.* **2001**, *63*, 871-894. (b) Wood, J. N.; Boorman, J. Voltage-gated sodium channel blockers; target validation and therapeutic potential. *Curr. Top Med. Chem.* **2005**, *5*, 529-537.

(3) Eijkelkamp, N.; Linley, J. E.; Baker, M. D.; Minett, M. S.; Cregg, R.; Werdehausen, R.; Rugiero, F.; Wood, J. N. Neurological perspectives on voltage-gated sodium channels. *Brain* **2012**, *135*, 2585-2612.

(4) (a) Dib-Hajj, S. D.; Yang, Y.; Black, J. A.; Waxman, S. G. The $Na_V1.7$ sodium channel: from molecule to man. *Nat. Rev. Neurosci.* **2013**, *14,* 49-62. (b) Lampert, A.; Eberhardt, M.; Waxman, S. G. Altered sodium channel gating as molecular basis for pain: contribution of activation, inactivation, and resurgent currents. *Handb. Exp. Pharmacol.* **2014**, *221*, 91-110. (c) Gingras, J.; Smith, S.; Matson, D. J.; Nye, D.; Couture, L.; Feric, E.; Yin, R.; Moyer, B. D.; Peterson, M. L.; Rottman, J. B.; Beiler, R. J.; Malmberg, A. B.; McDonough, S. I. Global $Na_V1.7$ knockout mice recapitulate the phenotype of human congenital indifference to pain. *PLoS ONE* **2014**, 9, e105895.

(5) (a) Fertleman C. R.; Baker M. D.; Parker K. A.; Moffatt S.; Elmslie, F. V.; Abrahamsen, B.; Ostman, J.; Kluqbauer, N.; Wood, J. N.; Gardiner, R. M.; Rees, M. SCN9A mutations in paroxysmal extreme pain disorder: allelic variants underlie distinct channel defects and phenotypes. *Neuron* **2006**, *52*, 767-774. (b) Yang Y.; Wang Y.; Li S.; Xu, Z.; Li, H.; Ma, L.;

Fan, J.; Bu, D.; Fan, Z.; Wu, G.; Jin, J.; Ding, B.; Zhu, X.; Shen, Y. Mutations in SCN9A, encoding a sodium channel alpha subunit, in patients with primary erythermalgia. *J. Med. Genet.* **2004**, *41,* 171-174. (c) Drenth J. P.; te Morsche R. H.; Guillet, G.; Taieb, A.; Kirby, R. L.; Jansen, J. B. SCN9A mutations define primary erythermalgia as a neuropathic disorder of voltage gated sodium channels. *J. Invest. Dermatol.* **2005**, *124*, 1333-1338.

(6) (a) Cox J. J.; Reimann F.; Nicholas A. K.; Thornton, G.; Roberts, E.; Springell, K.; Karbani, G.; Jafri, H.; Mannan, J.; Raashid, Y.; Al-Gazali, L.; Hamamy, H.; Valente, E. M.; Gorman, S.; Williams, R.; McHale, D. P.; Wood, J. N.; Gribble, F. M.; Woods, G. C. An SCN9A channelopathy causes congenital inability to experience pain. *Nature* **2006**, *444*, 894-898. (b) Goldberg Y. P.; MacFarlane J.; MacDonald M. L.; Thompson J.; Dube, M. P.; Mattice, M.; Fraser, R.; Young, C.; Hossain, S.; Pape, T.; Payne, B.; Radomski, C.; Donaldson, G.; Ives, E.; Cox, J.; Younghusband, H. B.; Green, R.; Duff, A.; Bolthauser, E.; Grinspan, G. A.; Dimon, J. H.; Sibley, B. G.; Andria, G.; Toscano, E.; Kerdraon, J.; Bowsher, D.; Pimstone, S. N.; Samuels, M. E.; Sherrington, R.; Hayden, M. R. Loss-of-function mutations in the $Na_V1.7$ gene underlie congenital indifference to pain in multiple human populations. *Clin. Genet.* **2007**, *71*, 311-319.

(7) Devigili, G.; Eleopra, R.; Pierro, T.; Lombardi, R.; Rinaldo, S.; Lettieri, C.; Faber, C. G.; Merkies, I. S. J.; Waxman, S. G. Paroxysmal itch caused by gain-of-function $Na_V1.7$ mutation. *Pain* **2014**, 5155*,* 1702-1707.

(8) (a) de Lera, R. M.; Kraus, R. L. J. Voltage-gated sodium channels: Structure, function, pharmacology, and clinical indications. *J. Med. Chem.* **2015**, *58*, 7093-7118. (b) King, G. F.; Vetter, I. No gain, no pain: $Na_V1.7$ as an analgesic target. *ACS Chem. Neurosci.* **2014**, *5,* 749-751. (c) Sun, S.; Cohen, C. J.; Dehnhardt C. M. Inhibitors of voltage-gated sodium channel $Na_V1.7$: patent applications since 2010. *Pharm. Pat. Anal.* **2014**, *3*, 509-521.

(9) (a) Beaudoin, S.; Laufer-Sweiler, M. C.; Markworth, C. J.; Marron, B. E.; Millan, D. S.; Rawson, D. J.; Reister, S. M.; Sasaki, K.; Storer, R. I.; Stupple, P. A.; Swain, N. A.; West, C. W.; Zhou, S. Sulfonamide derivatives. PCT Int. Appl. WO2010079443, Jul 15, 2010. (b) McCormack, K.; Santos, S.; Chapman, M. L.; Krafte, D. S.; Marron, B. E.; West, C. W.; Krambis, M. J.; Antonio, B. M.; Zellmer, S. G.; Printzenhoff, D.; Padilla, K.; M.; Lin, Z.; Wagoner, P. K.; Swain, N. A.; Stupple, P. A.; de Groot, M.; Butt, R. P.; Castle, N. A. Voltage sensor interaction site for selective small molecule inhibitors of voltage-gated sodium channels. *Proc. Natl. Acad. Sci. U.S.A.* **2013**, *110*, E2724-E2732.

(10) (a) Focken, T.; Liu, S.; Chahal, N.; Dauphinais, M.; Grimwood, M. E.; Chowdhury, S.; Hemeon, I.; Bichler, P.; Bogucki, D.; Waldbrook, M.; Bankar, G.; Sojo, L. E.; Young, C.; Lin, S.; Shuart, N.; Kwan, R.; Pang, J.; Chang, J. H.; Safina, B. S.; Sutherlin, D. P.; Johnson, Jr. J. P.; Dehnhardt, C. M.; Mansour, T. S.; Oballa, R. M.; Cohen, C. J.; Robinette, C. L. Discovery of aryl sulfonamides as isoform-selective inhibitors of $Na_V1.7$ with efficacy in rodent pain models. *ACS Med. Chem. Lett*. **2016**, *7*, 277-282. (b) Sun, S.; Jia, Q.; Zenova, A, Y,; Chafeev, M.; Zhang, Z,; Lin, S.; Kwan, R.; Grimwood, M. E.; Chowdhury, S.; Young, C.; Cohen, C. J.; Oballa, R. M; The discovery of benzenesulfonamide-based potent and selective inhibitors of voltage-gated sodium channel $Na_V1.7$. *Bioorg. Med. Chem Lett*, **2014**, *24*, 4397-4401.

(11) (a) Bell. A S.; Brown, A. D.; Lewthwaite, R. A.; Marsh, I. R.; Millan, D. S.; Pacheco, M. P.; Rawson, D. J.; Sciammetta, N.; Storer, R. I.; Stupple, P. A.; Swain, N. A.; de Groot, M. J. Chemical compounds. US. Pat. Appl. US20120010207, Jan 12, 2012. (b) Brown, A. D.; Rawson, D. J.; Storer, R. I.; Swain, N. A. N-sulfonylbenzamides as inhibitors of voltage-gated sodium channels. PCT Int. Appl. WO2012007868, Mar 8, 2012. (c) Brown, A. D.; Rawson, D.

J.; Storer, R. I.; Swain, N. J. Chemical compounds. PCT Int. Appl. WO2012007868, Jan 19, 2012.

(12) PX IC_{50} determinations were made using at least four different concentrations of test compound at half log units applied individually, with washout, recovery of current, and resetting of holding voltage between each individual concentration. Percent inhibition as a function of compound concentration was pooled from n = 5 different cells, with two to three data points per concentration, and fitting the resulting data set with a Hill (4-parameter logistic) fit in DataXpress 2.0 software to produce a single IC_{50} curve. See Experimental for complete details of protocols.

(13) Diaz, G. J.; Daniell; K.; Leitza, S. T.; Martin, R. L.; Su, Z.; McDermott, J. S.; Cox, B. F.; Gintant, G. A.; The [^{3}H]dofetilide binding assay is a predictive screening tool for hERG blockade and proarrhythmia: Comparison of intact cell and membrane preparations and effects of altering [K+]o. *J. Pharmacol. Toxicol. Methods* **2004**, *50*, 187– 199.

(14) (a) Marx, I. E.; Dineen, T. A.; Able, J.; Bode, C.; Bregman, H.; Chu-Moyer, M.; DiMauro, E. F.; Du, B.; Foti, R. S.; Fremeau, Jr. R. T.; Gao, H.; Gunaydin, H.; Hall, B. E., Huang, L.; Kornecook, T.; Kreiman, C. R.; La, D. S.; Ligutti, J.; Lin, M-H. J.: Liu, D.; McDermott, J. S.; Moyer, B. D.; Peterson, E. A.; Roberts, J. T.; Rose, P.; Wang, J.; Youngblood, B. D.; Yu, V.; Weiss, M. M. Heteroarylsulfonamides as selective $Na_V1.7$ inhibitors: optimizing potency and pharmacokinetics to demonstrate in vivo target engagement. Unpublished results. (b) Weiss, M.; DiMauro, E. F.; Dineen, T.; Graceffa, R.; Guzman-Perez, A.; Kreiman, C.; Marx, I. E.; Nguyen, H. N.; Peterson, E.; Deak, H. Bicyclic sulfonamide compounds as sodium channel inhibitors and their preparation. PCT Int. Appl. WO2014201173, Jun. 11, 2014. (c) Boezio, C.; Bregman, H.; Coats, J. R.; DiMauro, E. F.; Dineen, T.; Du, B.; Graceffa, R.; Kreiman, C.; La,

D.; Marx, I. E.; Chakka, N.; Nguyen, H-N.; Peterson, E. A.; Weiss, M.; Copeland, K.; Deak, H. L.; Boezio, A. Bicyclic aryl and heteroaryl sodium channel inhibitors. PCT Int. Appl. WO2013086229, Dec. 6, 2013. (d) Boezio, C.; Boezio, A.; Bregman, H.; Chakka, N.; Coats, J. R.; Copeland, K. W.; DiMauro, E. F.; Dineen, T.; Gao, H.; La, D.; Marx, I. E.; Nguyen, H-N.; Peterson, E. A.; Weiss, M. Dihydrobenzoxazine and tetrahydroquinoxaline sodium channel inhibitors. PCT Int. Appl. WO2013122897, Aug. 22. 2013. (e) Weiss, M.; Boezio, A.; Boezio, C.; Butler, J. R.; Chu-Moyer, M. Y.; DiMauro, E. F.; Dineen, T.; Graceffa, R.; Guzman-Perez, A.; Huang, H.; Kreiman, C.; La, D.; Marx, I. E.; Milgram, B. C.; Nguyen, H. N.; Peterson, E.; Romero, K.; Sparling, B. Bicyclic sulfonamide compounds as sodium channel inhibitors. PCT Int. Appl. WO2014201206, Dec. 18, 2014.

(15) (a) Hopkins A. L.: Keseru G. M.; Leeson P. D.; Rees D. C.; Reynolds C. H.; The role of ligand efficiency metrics in drug discovery. *Nat. Rev. Drug Discovery* **2014**, *13*, 105–121. (b) LipE was calculated using hNa_V1.7 PX IC_{50} and Amgen Na_V1.7 project cLogD(7.4). Amgen Na_V1.7 project cLogD(7.4) was calculated using daylight cLogP and an Amgen pK_a calculator, which was based on an empirical statistical in silico model derived using the Cubist statistical method and a pool of 820 molecular descriptors.

(16) For both heteroarylsulfonamdies and acyl sulfonamides, Amgen Na_V1.7 project cLogD(7.4) and calculated pK_a correlated well with measured LogD(7.4) (determined by high-throughput shake flask assay with in situ detection using nitrogen fluorescence detector) and measured pK_a (determined by UV spectrophotometry), respectively. Amgen calculated pK_a generally agreed with ACD calculated pKa and with measured pK_a by UV spectrophotometry. For example, measured pK_a: **1** = 3.13, **2** = 3.06.

(17) Jones, H. M.; Butt, R. P.; Webster, R. W.; Gurrell, I.; Dzygiel, P.; Flanigan, N.; Fraier, D.; Hay, T.; Iavarone, L. E.; Luckwell, J.; Pearce, H.; Phipps, A.; Segelbacher, J.; Speed, B.; Beaumont, K. Clinical micro-dose studies to explore the human pharmacokinetics of four selective inhibitors of human $Na_v1.7$ voltage-dependent sodium channels. *Clin. Pharmacokinet.* **2016**, *55*, 875-887.

(18) Berry, L. M.; Zhao, Z. An examination of IC_{50} and IC_{50}-shift experiments in assessing time-dependent inhibition of CYP3A4, CYP2D6 and CYP2C9 in human liver microsomes. *Drug Metab. Lett.* **2008**, *2*, 51−59.

(19) Bregman, H; Chakka, N.; DiMauro, E.; Gao, H.; Gunaydin, H.; Huang, H.; Olivieri, P.; Schenkel, L.; Weiss, M. Biaryl acyl-sulfonamide compounds as sodium channel inhibitors and their preparation. PCT Int. Appl. WO2015051043 Apr. 9, 2015.

(20) Davies, B.; Morris, T. Physiological parameters in laboratory animals and humans. *Pharm. Res*. **1993**, *10*, 1093–1095.

(21) Galetin, A. Rationalizing underprediction of drug clearance from enzyme and transporter kinetic data: from in vitro tools to mechanistic modeling. *Methods Mol. Biol.* **2014**, *1113*, 255-288.

(22) Sohlenius-Sternbeck, A-K.; Fagerholm, U.; Bylund, J. The volume of distribution is an indicator of poor *in vitro–in vivo* extrapolation of clearance for acidic drugs in the rat. *Xenobiotica* **2013**, *43*, 671-678.

(23) Madeja, M. Do neurons have a reserve of sodium channels for the generation of action potentials? A study on acutely isolated CA1 neurons from the guinae-pig hippocampus. *Eur. J. Neurosci.* **2000**, *12*, 1-7.

(24) Morgan, R. E.; Trauner, M.; van Staden, C. J.; Lee, P. H.; Ramachandran, B.; Eschenberg, M.; Afshari, C.; Qualls, C. W. Jr.; Lightfoot-Dunn, R.; Hamadeh, H. K. Interference with bile salt export pump function is a susceptibility factor for human liver injury in drug development. *Toxicol. Sci.* **2010**, *118*, 485-500.

(25) ^{3}H-heteroaryl-sulfonamide: (P)- 1-(3'-chloro-2-fluoro-5,5'-dimethoxy-[1,1'-biphenyl]-4-yl)-N-(isoxazol-3-yl)-2-oxo-1,2-dihydroquinoline-6-sulfonamide [5'-methoxy-$C^{3}H_{3}$]; based on compound 501 in reference 14d.

(26) Ahuja, S.; Mukund, S.; Deng, L.; Khakh, K.; Chang, E.; Ho, H.; Shriver, S.; Young, C.; Lin, S.; Johnson, J. P.; Wu, P.; Li, J.; Coons, M.; Tam, C.; Brillantes, B.; Sampang, H.; Mortara, K.; Bowman, K. K.; Clark, K. R.; Estevez, A.; Xie, Z.; Verschoof, H.; Grinwood, M.; Dehnhardt, C.; Andrez, J-C.; Focken, T.; Sutherlin, D. P.; Safina, B. S.; Starovasnik, M. A.; Ortwine, D. F.; Franke, Y.; Cohen, C. J.; Hackos, D. H.; Koth, C. M.; Payandeh, J. Structural basis of $Na_V1.7$ inhibition by an isoform-selective small-molecule antagonist. *Science* **2015**, *350*, aac5464:1-9.

(27) Tan, H.; Semin, D.; Wacker, M.; Cheetham, J. An automated screening assay for determination of aqueous equilibrium solubility enabling SPR study during drug lead optimization. *JALA* **2005**, *10*, 364−373.

(28) Huang, L.; Berry, L.; Ganga, S.; Janosky, B.; Chen, A.; Roberts, J.; Colletti, A. E.; Lin, M. H. Relationship between passive permeability, efflux, and predictability of clearance from in vitro metabolic intrinsic clearance. *Drug Metab. Dispos.* **2010**, *38*, 223−231.

Table of Contents artwork

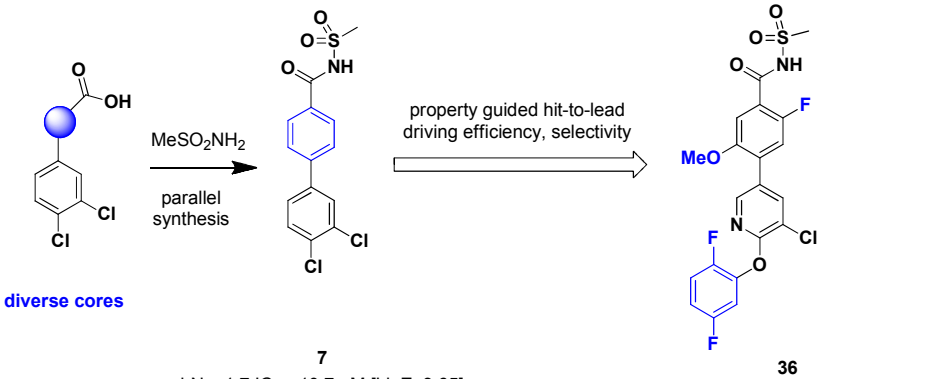

7

$hNa_V1.7$ IC_{50}: 10.7 μM [LipE: 3.65]

$hNa_V1.5$ IC_{50}: >42 μM

36

$hNa_V1.7$ IC_{50}: 0.050 μM [LipE: 6.5]

$hNa_V1.5$ IC_{50}: 11.9 μM